PRELIMINARY STUDIES OF THE INFLUENCE OF FORCES AND KINETICS ON INTERFACIAL COLLOIDAL ASSEMBLY

A Thesis

by

GREGORY FERNANDES

Submitted to the Office of Graduate Studies of
Texas A&M University
in partial fulfillment of the requirements for the degree of

MASTER OF SCIENCE

August 2004

Major Subject: Chemical Engineering

PRELIMINARY STUDIES OF THE INFLUENCE OF FORCES AND KINETICS ON INTERFACIAL COLLOIDAL ASSEMBLY

A Thesis

by

GREGORY FERNANDES

Submitted to Texas A&M University
in partial fulfillment of the requirements
for the degree of

MASTER OF SCIENCE

Approved as to style and content by:

Michael Bevan (Chair of Committee)	David Ford (Member)
Kenneth Hall (Head of Department)	Richard Crooks (Member)

August 2004

Major Subject: Chemical Engineering

ABSTRACT

Preliminary Studies of the Influence of Forces and
Kinetics on Interfacial Colloidal Assembly. (August 2004)
Gregory Fernandes, B.E., Mumbai University
Chair of Advisory Committee: Dr.Michael Bevan

In this research we illustrate how particle-particle and particle-substrate interactions affect structure in interfacial colloidal systems. A number of tools are used to quantify characteristics of deposited structures. These results help understand the effects of colloidal system interactions and deposition kinetics on the degree of ordering in interfacial colloidal structures.

The first set of experiments involve 2.34 μm silica colloids interacting with silica substrates in 0mM, 5mM, 10mM, and 100mM NaCl solutions. Only the 100mM NaCl solution resulted in rapid deposition driven by van der Waals attraction, while residual electrostatic repulsion produced levitation at lower ionic strengths. This allowed direct observation of the effects of varying magnitudes of attractive interactions on interfacial colloidal structures. Rapid deposition of positively charged 1μm latex colloids on negatively charged silica substrates driven by Coulombic and van der Waals attraction produced surface structures similar to those obtained with only van der Waals attraction. Experiments on 2.34 μm silica colloids interacting with silica substrates in 10mM NaCl/pH 5.5 and 10mM NaCl/pH 10 conditions resulted in slower deposition rates. It was also found that slower deposition rates produced more compact structures displaying a higher degree of order.

Another set of experiments was aimed at understanding interactions and structures formed in systems of polymerically levitated particles. Total internal reflection microscopy (TIRM) experiments revealed the influence of underlying

substrate chemistry on interaction profiles in these systems. Basic experiments were also performed on the effects of varying amounts of specific ions on the dispersion stability in these systems. At conditions producing instability in polymeric systems, a similar degree of order was observed in comparison to experiments involving rapid deposition via salt addition in electrostatically stabilized systems.

The results of this research clearly indicate that particle-particle and particle-substrate interactions are critical in determining structure formation by deposition. While the principal focus of this research is to study structures formed in various kinetic regimes, it also provides a basis for future studies aimed at tuning attractive interactions to produce equilibrium colloidal crystals on substrates.

Many thanks to my parents

ACKNOWLEDGMENTS

I acknowledge, with gratitude, the support of the many people, who have, in even the smallest way helped me get through the past two years. Many thanks to my parents, my brother John and cousins Siddharth, Rohan, Samantha and Robert who have supported me all the way. I owe a big thank you to my wonderful advisor, Dr. Michael A. Bevan, who has been for me a source of knowledge and encouragement throughout. I would like to thank my committee members, Dr. David Ford and Dr. Richard Crooks.

A big thank you to Towanna without whom I would literally not have been in a position to graduate. Thank you, Samartha and Wu, the best research mates anyone could ask for. Li Sun, I greatly appreciate the time you invested in helping me with microcontact printing.

I would like to thank all my friends who made my stay here a most enjoyable one. I would especially like to thank my dear friends (This might take a while!) Anita Rego, Ajay Bijoor, Akshay Kirtikar, Sagar Kale, Mahesh Bhoj, Hardik Sheth, Kunal Chokshi, Omkar Joshi, Anjan Ghosh, Sandeep Sachdeva, Vishal Karnik, Jyotpal Panesar, Barjinder Gharcha, Amit Goel, Hans Kumar, Sanjay Tiwari, Vipin Tyagi, Arnab Chakrabarty, Amit Sahu, Sumit Sharma, Abhay Singh, Pardeep Brar, Udit Budhia, Vijay Teenarsipur, Vijay Raghunathan, Faisal Shaikh, Mert Atilhan, Jagdish Rao, Jui Gadade, Manmeet Vedi, Suhas Verma, Sumit Kumar, Srinivas Cherla, Prashanth Nittala, Amar Phiroze, Pradip Bahukudumbi, Francis Sebastian, Hayley McCardle, Hayley Lebsock, Mike Delaney, Brian Simmons, Jardin Simpson, Travis Gregg, Holly Catanach, Katy Burggraf, Katrina Ohmes, Heidi Threadgil, Lucas Folegatti and the rest of the gang.

TABLE OF CONTENTS

Page

ABSTRACT iii

DEDICATION v

ACKNOWLEDGMENTS vi

TABLE OF CONTENTS vii

LIST OF FIGURES x

LIST OF TABLES xiii

1. THESIS INTRODUCTION 1

    1.1 Objectives & significance 1
    1.2 Historical perspective 2
    1.3 Recent literature review 3
        1.3.1 Colloidal assembly 3
        1.3.2 Chemical templates and their applications to colloidal deposition 4
        1.3.3 Adsorbing polymer systems 4
        1.3.4 Force measurements using TIRM 5
    1.4 Summary of Conclusions 5

2. THEORY 7

    2.1 Colloidal forces 7
        2.1.1 Hydrodynamics 7
        2.1.2 Brownian motion 7
        2.1.3 Van der Waals interactions 8
        2.1.4 Electrostatics 9
        2.1.5 Polymeric forces 10
    2.2 Fractal dimension 10
    2.3 Fuchs stability ratio 11
    2.4 Triangulation 13
    2.5 Radial distribution function 14
    2.6 Total internal reflection microscopy (TIRM) 15

3. EXPERIMENTAL 17

    3.1 Stamp fabrication and micro-contact printing 17
    3.2 Polystyrene spin coating 18
    3.3 Cell preparation 18
    3.4 Polymer adsorption 18
    3.5 Confocal experiments 19
    3.6 TIRM experiments 20

Page

4. DIFFUSION LIMITED DEPOSITION 21

4.1 Introduction 21
4.2 Theory 22
4.2.1 Fractal dimension: evaluation and interpretation 22
4.2.2 Bond orientational order parameter, radial distribution function and triangulation 24
4.2.3 Fuchs stability ratio 25
4.3 Experimental 27
4.3.1 Materials 27
4.3.2 Cell preparation 27
4.3.3 Confocal imaging 28
4.3.4 Procedure 28
4.4 Results and discussion 28
4.4.1 Surface structure in silica particles on glass as a function of ionic strength 28
4.4.2 Surface structure in amidine terminated latex particles on glass 34
4.5 Conclusions 36

5. REACTION LIMITED DEPOSITION 38

5.1 Introduction 38
5.2 Experimental 40
5.2.1 Materials 40
5.2.2 Cell preparation 40
5.2.3 Confocal imaging 41
5.2.4 TIRM analysis 41
5.2.5 Procedure 41
5.3 Results and discussion 42
5.3.1 Measurement of pH dependent deposition and structure on silica substrates (CLSM studies) 42
5.3.2 Measurement of pH dependent deposition and structure on silica substrates (TIRM studies) 45
5.4 Conclusions 47

6. LEVITATION & DEPOSITION WITH POLYMERIC FORCES 49

6.1 Introduction 49
6.2 Theory 50
6.2.1 Polymeric stabilization 50
6.2.2 Silica surface modification using silane chemistry 51
6.2.3 Specific ion effect 51
6.3 Experimental 52
6.3.1 Materials 52

Page

6.3.2 Cell preparation 52
6.3.3 Surface modification with PS 53
6.3.4 Surface modification with OTS 53
6.3.5 TRIM studies 53
6.3.6 Confocal imaging 54
6.3.7 Procedure 54
6.4 Results and discussion 54
6.4.1 Effect of substrate properties on polymeric stabilization (TIRM studies) 54
6.4.2 Predicting diffusion limited deposition and aggregation 59
6.5 Conclusion 62

7. CONCLUSIONS 63

7.1 Summary 63

8. FUTURE RESEARCH 65

8.1 Diffusing colloidal probe microscopy (DCPM) 65
8.2 Specific ion effects on polymer mediated interfacial structures 66
8.3 Manipulation of self-assembly on chemical templates 68
8.4 Protein interaction measurements 69
8.5 Combinatorial microarray experiments 69

REFERENCES 70

VITA 73

LIST OF FIGURES

FIGURE Page

2.1 Particle-wall squeeze flow and particle-particle squeeze flow 13

2.2 Radial distribution function for liquid argon showing typical liquid like structure 14

2.3 Schematic diagram showing particle scattering evanescent wave in TIRM 16

4.1 Sample images of diffusion limited aggregates of (L-R) 256, 512 & 1024 particles respectively used for verification of the fractal dimension program ... 23

4.2 Triangulation (Image and histogram) for 2.34μm silica spheres on silica surface at 5mM NaCl 24

4.3 Fuchs Stability Ratio for rapid flocculation of PS lattices in water as a function of sphere radius generated by use of MathCAD worksheet and equations (2.3, 2.11, 2.13) 26

4.4 The onset of diffusion-limited kinetics for a system of 2.34μm silica spheres interacting with silica substrate generated using MathCAD spreadsheet and equations (2.11, 2.12, 2.14) 26

4.5 Influence of rapid deposition kinetics on structural characteristics of 2.34μm deposited silica particles 29

4.6 Radial distribution functions for 2.34μm silica particles on silica substrate at (L-R): 0mM, 5mM, 10mM, and 100mM salt concentrations respectively 31

4.7 Triangulation histograms for a system of 2.34μm silica particles on silica substrate at 5mM, 10mM, and 100mM salt concentrations respectively 33

4.8 Radial distribution functions and triangulation analysis for diffusion limited deposition of positively charged 1μm amidine terminated latex colloids on negative glass surface 35

4.9 Radial distribution functions for diffusion limited deposition of positively charged colloids on glass surface (closed dots, predominant attractive force is electrostatic) and diffusion limited deposition of silica spheres on glass at high ionic strength (open dots, predominant attractive force is van der Waals)

FIGURE Page

where each data set is normalized by the separation at the first peak (particle diameter)..... 37

5.1 Importance of repulsive energy barrier, a kinetic barrier associated with electrostatics..... 39

5.2 Radial distribution functions for pH=5.5 and pH=10 43

5.3 Triangulation histograms for pH=5.5 (Top) and pH=10 (Bottom) clearly show a sharpening of the peak..... 44

5.4 The interaction potential between a 2.34μm silica particle and a glass substrate at 10mM NaCl and pH 10 in terms of relative separation (nm) with (L) and without gravity (R)..... 46

5.5 The interaction potential between a 2.34μm silica particle and a glass substrate at 10mM NaCl and pH 10 in terms of absolute separation (nm) 47

5.6 Reaction limited deposition structures (black triangles) show higher values of fractal dimensions than structures formed by diffusion-limited deposition (gray triangle)..... 48

6.1 Polymeric Stabilization 50

6.2 (L-R) Interaction potentials for PS-PS and PS-OTS cases clearly show a decrease in the attractive well depth 55

6.3 (Top) Fitting for PS-PS interaction data with gravity (L) and without (R)..... 57

6.4 The relevant separations in polymeric stabilization showing layer thickness and bare surface separations..... 58

6.5 Interaction potentials for PS-PS (gray dash) and PS-OTS (black) showing the shifting of hard wall repulsion 59

6.6 Predicting rapid-deposition from particle-wall interaction potential 60

6.7 Bulk aggregation experiments at performed at (L-R) 0.5M NaCl, 0.25M NaCl+0.25M $MgSO_4$ and, 0.5M $MgSO_4$ clearly showing aggregation at 0.5M $MgSO_4$ as predicted 61

FIGURE Page

6.8 (L) Surface structure (represented by g(r)) for a PS particle on OTS diffusion limited deposition structure showing the typical random nature of such structures 61

8.1 Diffusing Colloidal Probe Microscopy (DCPM) on a simple heterogeneous surface 67

8.2 Previous work on phase transition in polymerically stabilized systems 68

LIST OF TABLES

TABLE Page

4.1 Performance of Fortran fractal program 24

4.2 Effect of ionic strength on structure of deposited colloidal layers 28

4.3 Deviation from crystallinity with increase in ionic strength 31

4.4 Poor ordering due to large electrostatic attraction 34

5.1 Change of solvent conditions in reaction-limited regime to achieve higher amounts of order 43

6.1 Influence of underlying substrate chemistry on the attractive well depth in polymerically stabilized systems 55

6.2 Influence of substrate chemistry 58

6.3 Influence of substrate properties 58

1. THESIS INTRODUCTION

1.1 Objectives and significance

The broad goal of the proposed work is to understand how colloidal interactions influence assembly processes. The central question related to attaining these objectives is an understanding of how particle-particle and particle-substrate interactions, mediated by solvent conditions, affect the kinetics of colloidal assembly processes. This research takes a step in that direction by using a combination of Total Internal Reflection Microscopy (TIRM) and confocal laser scanning microscopy (CSLM) to understand and quantify the effects of subtle variations in interaction on assembled structures.

In this research we focus on two systems in our efforts to understand the effects of interactions and kinetics on interfacial colloidal structures. The first of these is a charge-stabilized system. The objective is to induce instability in these systems by either removing repulsion or adding attraction and then observe the resulting deposited structures. The aim here is to study two distinct deposition regimes, rapid and slow. As with previous studies done on aggregates[1-4], the goal is to be able to explain the packing characteristics of resulting structures by a fundamental knowledge of the particle-particle and particle-substrate interactions. The desire is to be able to predict the type of structures expected form knowledge of solvent conditions, which directly determine system interactions and substrate properties.

The other system of interest in this study is a sterically stabilized system. The focus of this part of the research is to gain an insight into the nature of forces and interactions in these systems. We want to study and measure the effects of substrate

---

This thesis follows the style of *Langmuir*.

chemistry and solvent conditions on the interactions in sterically stabilized colloidal systems. Since the variation of adsorbed polymer layer thickness (attractive well depth) with specific ion concentrations is known[5], we can use the knowledge gained from the first part of the research to get some preliminary insights into solvent conditions that cause system instability.

Though the main focus of the research is studying structures formed under various kinetic regimes, it forms an important background for any study related to the assembly of perfect crystals. By studying all regimes of colloidal deposition, it throws light on those conditions that are conducive to phase transition. The work done on polymerically stabilized systems also serves an important purpose as such systems produce reversible effects[6], allow for exquisite interaction tuning[7] and therefore form excellent systems for crystal growth studies. Since this research isolates regions of colloidal system stability and instability, it provides an ideal starting point for such research.

1.2 Historical perspective

The first observations of colloidal flocculation were by Faraday who noticed rapid, irreversible flocculation in systems of colloidal gold sol on addition of salt. Shultz (1882) and Hardy (1900) later justified this by elucidating the role of added electrolytes in suppressing the effects of charge and inducing flocculation. After it was known that dispersions could be flocculated by screening the electrostatic repulsion, Smoluchowski (1917) deduced expressions for the rate of formation of small aggregates by Brownian and shear-induced collisions. In order to study colloidal stability, a representation of the interparticle potential was most crucial. A representation of total interparticle potential as the sum of attractive and repulsive components was an important development in the theory of colloidal stability. Work by Derjaguin and Landau (1941) and, Verwey and Overbeek (1948) led to the development of this theory called the DLVO theory.

The synthesis of model colloids by Vanderhoff (1956), Matijevic (1976) and Iler (1979) removed complications due to polydispersity and enabled theories of flocculation

to be tested clearly. The need to disperse particles at high ionic strengths or in non-aqueous solvents led to improved techniques for polymeric stabilization in the 1960s. The development of block and graft copolymers revolutionized the process. These molecules combined an insoluble component for attachment to the particle surface and a soluble chain for stabilization. The pioneering work of Napper (1983) revealed the relation between the stability of the dispersion and the solution properties of the stabilizing block.[8,9]

1.3 Recent literature review

1.3.1 Colloidal assembly

Colloidal systems have been studied extensively by physicists to gain an understanding into phase transitions. Suspensions of uniform colloidal particles, which are good approximations to hard spheres, have been extensively used to provide an experimental model system for investigating hard-sphere systems. It has been found that while the most thermodynamically favorable state for these systems is the crystalline state, the influence of gravity leads to the formation of a metastable glass state. An important study in microgravity conditions justified this view.[10,11]

Equilibrium thermodynamics predicts the occurrence of crystals as the stable thermodynamic phase upon crossing the solubility boundary. The formation of glasses and gels has been attributed to purely kinetic phenomena.[12,13] Studies conducted on systems with large attractive interactions showed the formation of kinetically trapped structures like aggregates. [14-18] It was found that fractal theory provided a good description of the morphology of structures formed during the two-dimensional and three-dimensional aggregation.

An important development in this area was the isolation of reaction limited and diffusion limited regimes of irreversible colloid aggregation. Lin et al. (1989) investigated the aggregation of three chemically different colloidal systems under both reaction-limited and diffusion-limited conditions and suggested that each limiting regime

was universal, independent of the chemical details of the particular colloid system. Various groups have done considerable work on this subject since then.[1-4]

1.3.2 Chemical templates and their applications to colloidal deposition

Whitesides and Kumar (1993) described a technique for producing patterned self-assembled monolayers (SAMs) with geometrically well-defined regions of different chemical functionality and thus different physical and chemical properties. This technique, microcontact printing, uses an elastomeric 'stamp' and alkanethiol 'ink' to form patterned SAMs of alkanethiolates on gold films with dimensions ranging from 200 nm to several cm.[19-21] They also applied this method to pattern SAMs of silanes on glass.[22] Several other groups have suggested slight variations in the original process.[23,24]

Recent applications of microcontact printing involve studies in which multilayers of polyelectrolyte were deposited on chemically patterned surfaces.[25] The polyelectrolyte was used to provide a platform on which colloids are strongly bound by electrostatic attraction. Another important paper in this area is one by Aizenberg, Braun and Wiltzius (2000) in which charged colloidal particles were deposited on chemically micropatterned substrates with anionic and cationic regions.[26] Opposite charge attraction between monolayers of microcontact printed silanes and silica spheres have been used to generate low-dimensional arrangements of colloidal particles.[27] All these studies are examples of assembly of colloidal structures by diffusion-limited deposition. Though such deposition experiments have been conducted, no effort has been made to systematically study the kinetic aspects and system interactions that result in the formation of such structures.

1.3.3 Adsorbing polymer systems

Bevan and Prieve have done a good amount of work on polymerically stabilized systems. Using TIRM and light scattering techniques Bevan has measured interactions and isolated critical flocculation temperatures in these systems. The stabilizing polymer used was Pluronic triblock (PEO-PPO-PEO) with a PPO anchor block and two PEO tails extending into the solution as the stabilizing moiety.[6,7,28-31] These systems allow both

attractive and repulsive interactions to be induced. The effects in these systems are reversible which allows annealing of surface structures formed by these systems till surface defects are eliminated. The other advantage of the adsorbing polymer systems is that attraction can be localized on particles and surfaces.

1.3.4 Force measurements using TIRM

Prieve et al. (1987) developed a technique, which performed ultra sensitive measurements of colloidal interactions. Using TIRM it is possible to monitor the separation distance between a single microscopic sphere immersed in an aqueous solution and a transparent plate. Because the distance is calculated from the intensity of light scattered by the sphere when illuminated by an evanescent wave, this technique provides a sensitive, non-intrusive, and instantaneous measure of the distance between the sphere and the plate. Changes in distance as small as 1 nm can be detected. From the equilibrium distribution of separation distances sampled by Brownian motion, the potential energy profile in the vicinity of the minimum formed by gravitational attraction and double-layer repulsion or steric repulsion caused by an adsorbed soluble polymer can be determined. Van der Waals attraction, the radiation pressure exerted by a focused laser beam, receptor-mediated interaction between antigen and antibodies, and steric repulsion due to adsorbed polymer layers have been successfully measured with TIRM.[32-34]

1.4 Summary of conclusions

In this research we have successfully shown that like in aggregation studies conducted earlier[1], the particle-particle and particle-substrate interactions can be used to fundamentally explain the nature of structures formed by colloidal deposition at liquid-solid interfaces. This study shows that in systems that are initially charge stabilized, two distinct types of deposition kinetics are possible. For cases where the net interaction potential between particle and substrate is attractive, diffusion limited kinetics govern, which result in the formation of structures that are different form those formed in the presence of a surmountable repulsive barrier (reaction limited deposition). An important

observation in our studies is that like in aggregation, the diffusion limited kinetic regime is universal, independent of the chemical details of the particular colloid system.

The research also studies polymerically stabilized systems. An in depth understanding of substrate properties on adsorbed layer thickness is obtained. The nature of the particle-particle and particle-substrate interactions is studied in detail and measured by use of TIRM. Previous unpublished studies indicate the effect of specific ions on the polymer layer thickness (and particle-particle and particle-substrate interaction). Various specific ion concentrations are used and it is found that at 0.5M of $MgSO_4$, aggregates begin to form in the bulk of these systems. Deposition at these solvent conditions is diffusion-limited and the resulting surface structures display the same random packing characteristics observed in previous studies on this kinetic deposition regime.

2. THEORY

2.1 Colloidal forces

2.1.1 Hydrodynamics

It is a dynamical effect that arises when particles move in a liquid medium. As a unit moves, it creates a flow in the surrounding incompressible liquid. The presence of a second particle will influence the flow patterns in the liquid and will result in the two particles seeing each other through the flow of the intervening fluid. This effect is called the hydrodynamic interaction.

An important concept, which will be used in this research, is one of two spheres translating through a quiescent fluid. Hydrodynamic correction factors used in Fuchs stability ratio calculations are obtained from hydrodynamic interactions for particle-particle and particle-wall squeeze flow. The expression of hydrodynamic interaction for particle-particle squeeze flow is given by:

$$G(l) = \frac{54(l/a)^3 + 71(l/a)^2 + 8(l/a)}{54(l/a)^3 + 154(l/a)^2 + 60(l/a) + 4} \tag{2.1}$$

and for particle-wall squeeze flow is given by:

$$G(l) = \frac{6(l/a)^2 + 2(l/a)}{6(l/a)^2 + 9(l/a) + 2} \tag{2.2}$$

where *G(l)* is the hydrodynamic interaction for two spheres of radius *a* approaching each other or a sphere of radius *a* approaching a wall. The surface separation is represented by *l*.[8]

2.1.2 Brownian motion

A liquid that is totally homogeneous on a macroscopic scale undergoes continuous fluctuations at the molecular level. As a result of these fluctuations, the density of molecules at any location in the liquid varies with time and at any time varies with location in such a way that the mean density of the sample as a whole has its bulk value. This pattern of "flickering" molecular densities will produce continually varying

pressures on the surface of any particle submerged in the liquid. Since the fluctuations are confined to domains of the order of molecular dimensions, this randomly variable pressure is quite small. A small particle will be displaced, however, by the resulting force unbalance at its surface. The pattern of its displacements will also be totally random, a refection of the fluctuations which cause the motion. Such movements are called Brownian motion.[35]

2.1.3 Van der Waals interactions

Atoms with fluctuating dipoles polarize nearby atoms and the time averaged interaction between these two atoms is attractive. The potential of this attractive force is known as the dispersion (London) energy. Molecules with permanent dipole undergo Brownian rotation. They don't have a time-averaged dipole moment because of this but a correlation with other Brownian dipoles results in a time averaged attractive energy called Keesom energy. Neutral atoms can acquire an induced dipole from interaction with a molecule with a permanent dipole. The correlation between instantaneous dipoles also leads to a net attraction known as the induction (Debye) energy. All these interaction energies decay as the negative sixth power of the center-to-center distance between the atoms. All these energies collectively constitute the van der Waals interaction energy.

In 1937, H. C. Hamaker computed the van der Waals interaction between two particles of a condensed phase by linearly superimposing the atom-atom interactions. This ignores the effect of intervening atoms on the correlation between the two interacting dipoles. In 1955, E. M. Lifshitz devised a continuum theory to calculate the van der Waals interaction between condensed phases. While the van der Waals interaction between two atoms separated by a vacuum is always attractive, the interaction between two half spaces composed of different materials, separated by a third material, can be either attractive or repulsive, depending on the relative dielectric spectra of the three materials.[29]

The van der Waals interaction potential measured for two 360nm PS spheres interacting across water with 0.5M NaCl is given by:

$$\phi_{vdw,PS}(l,a) = \frac{489.9 - 8.917l + 0.1221l^2 - (5.236\times10^{-4})l^3}{1 + 13.08l + 1.017l^2 + 0.01530l^3} \qquad (2.3)$$

where l is the surface separation in nm. This equation needs to be adjusted for any PS particle with radius *a (nm)* interacting with a PS surface:

$$\phi_{vdw,PS}(l,a) = 2\left\{\frac{489.9 - 8.917l + 0.1221l^2 - (5.236\times10^{-4})l^3}{1 + 13.08l + 1.017l^2 + 0.01530l^3}\right\}\frac{a}{180} \qquad (2.4)$$

The equations represented here are fits to the values provided by the Lifshitz theory. The equation for a silica sphere of radius *a (nm)* interacting with a silica surface across water is similarly given by: [7]

$$\phi_{vdwS}(l,a) = -2409.6925\left(\frac{a}{1150}\right)(l)^{-2.1543} \qquad (2.5)$$

2.1.4 Electrostatics

The charging of a surface in a liquid can come about either by the ionization of surface groups or by the adsorption of ions from the solution onto a previously uncharged surface. Whatever the charging mechanism, the final surface charge is balanced by an equal but oppositely charged region of counterions, some of which are bound, usually transiently, to the surface within the so-called Stern layer, while others form an atmosphere of ions in rapid thermal motion close to the surface, known as the diffuse electrical double layer.[36]The electrostatic potential (Derjaguin approximation with non-linear superposition result) for spheres of radius a interacting with a surface is given by:

$$\phi_{elec}(l,C) = \frac{1}{kT}\left[64\pi a\varepsilon\left(\frac{kT}{e_0}\right)^2 \tanh\left(\frac{e_0\psi_1}{4kT}\right)\tanh\left(\frac{e_0\psi_2}{4kT}\right)\right]e^{(-\kappa(C)l)} \qquad (2.6)$$

where C is the salt concentration, a is particle radius, ψ's are surface potentials, l is surface separation, ε is the permittivity of the medium and κ is the Debye length. For the case of two spheres, the potential is adjusted by a factor of ½.

2.1.5 Polymeric forces

Adsorbed polymer layers have a certain brush thickness, which is dependent on the solvent quality. When two polymer brushes make contact, there is hard wall repulsion. Polymer layers also contribute to van der Waals interactions. For PS particles with Pluronic adsorbed on them, the modified van der Waals interaction is given by:

$$\phi_{vdw,PS}(l,a) = \left(\frac{-28.97 + 39.02l - 0.4759l^2 + (1.6\times10^{-3})l^3}{1 - 0.9158l + 0.0736l^2 + 0.0577l^3} \right) \frac{a}{180} \qquad (2.7)$$

For the case where a Pluronic coated PS particle is interacting with a Pluronic coated PS surface, the van der Waals interaction is adjusted by a factor of 2.[7]

2.2 Fractal dimension

The measurement of the 'size' of a set of points in space gives an idea of its dimension. A curve can be measured by finding the number $N(\delta)$ of line segments of length δ needed to cover it. The length of the curve is given by $L = N(\delta)\delta \rightarrow L_0\delta^0$ (as $\delta \rightarrow 0$). In the limit $\delta \rightarrow 0$, the measure L becomes asymptotically equal to the length of the curve and is independent of δ. Area can also be associated with the set of points defining a curve by giving the number of disks or squares needed to cover the curve. The number of squares is $N(\delta)$, and each square has an area of δ^2. The associated area is given by $A = N(\delta)\delta^2 \rightarrow L_0\delta^1$ (as $\delta \rightarrow 0$). Volume may be associated with the line too. $V = N(\delta)\delta^3 \rightarrow L_0\delta^2$ (as $\delta \rightarrow 0$). For ordinary curves both A and V tends to zero as δ vanishes, and the only interesting measure is the length of the curve. A line or simple curve is therefore a one-dimensional object. The only useful measure of a set of points defined by a surface in three-dimensional space is the area. A surface is therefore a two-dimensional object.

A set of points that is a curve which twists so badly that its length is infinite and fills the plane will have a dimension between one and two. There are also surfaces that fold so wildly that they fill space. Such strange sets of points have fractions of a dimension or non-integer dimensions and are called fractals.[37] Fractal dimension is a direct measure of the amount of order in an image. An infinite sheet made up of hexagonally close packed colloids would have a fractal dimension of two. An image, which shows poor packing, will obviously have a fractal dimension lesser than two.

It is already known from literature that for two-dimensional clusters formed by diffusion-limited kinetics, the value of fractal dimension is around 1.44 ± 0.04.[2-4] Knowledge of the radius of gyration (R_g) and the number of particles in a cluster (N) along with particle radius (R_p) is sufficient for obtaining the fractal dimension (D_f). The equations[38] used are:

$$N = \left(\frac{R_g}{R_p} \cdot \frac{1}{\sqrt{\frac{D_f}{D_f + 2}}} \right)^{D_f} \tag{2.8}$$

$$R_g = \left(\frac{\sum_i m_i \{(x_i - x_{cm})^2 + (y_i - y_{cm})^2\}}{\sum_i m_i} \right)^{\frac{1}{2}} \tag{2.9}$$

$$x_{cm} = \frac{\sum_i m_i x_i}{\sum m_i}, y_{cm} = \frac{\sum_i m_i y_i}{\sum m_i} \tag{2.10}$$

2.3 Fuchs stability ratio

Dispersion forces acting between similar particles suspended in a chemically different liquid are generally attractive. This provides a driving force toward macroscopic phase separation. The maintenance of a dispersed phase requires an opposing interparticle repulsion, achieved in this section through electrostatic forces. At high ionic strengths the electrostatic repulsion becomes insignificant and the interparticle

potential reduces to that of dispersion effects alone. Fuchs stability ratio is a measure of the degree of stability in a colloidal system. It is comparison of the rapid rate of aggregation (if only attractive interactions exist between particles) with the actual rate of aggregation in the system (with the actual interactive potential). The expression for Fuchs Stability Ratio is:

$$W = 2a \int_{0}^{1000a} \frac{e^{\left(\frac{\phi}{kT}\right)}}{(l+2a)^2 G(l)} dl \tag{2.11}$$

where a is the particle radius, *l* is the surface-to-surface separation between the particles *G (l)* is the hydrodynamic correction factor for two spheres approaching each other and ϕ is the interaction potential between the colloids.[8]

For particle-wall squeeze flow, shown in Figure 2.1 the equation is:

$$G(l) = \frac{6(l/a)^2 + 2(l/a)}{6(l/a)^2 + 9(l/a) + 2} \tag{2.12}$$

whereas for particle-particle squeeze flow, Figure 2.1 the equation is :

$$G(l) = \frac{54(l/a)^3 + 71(l/a)^2 + 8(l/a)}{54(l/a)^3 + 154(l/a)^2 + 60(l/a) + 4} \tag{2.13}$$

The particle-wall interaction potential ϕ for silica particle-silica surface (obtained by DLVO) is:

$$\phi(l,a,C) = \frac{1}{kT}\left[64\pi a\varepsilon\left(\frac{kT}{e_0}\right)^2 \tanh\left(\frac{e_0\psi_1}{4kT}\right)\tanh\left(\frac{e_0\psi_2}{4kT}\right)\right]e^{(-\kappa(C)l)} - 2.41\times10^3\left(\frac{a}{1150}\right)(l)^{-2.1543} \tag{2.14}$$

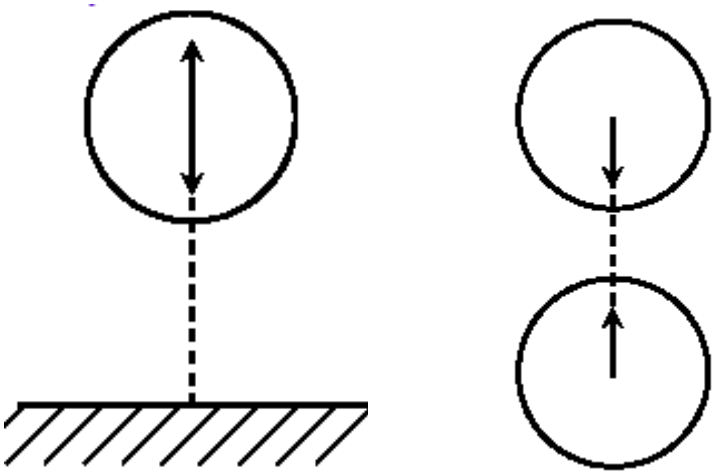

Figure 2.1. Particle-wall squeeze flow and particle-particle squeeze flow.

2.4 Triangulation

Triangulation is a subdivision of the plane into triangles, hence the name. The images analysed in this research are a set of points (particle centres) on a plane. The triangulation algorithm used here draws lines between every particle center in the image. The shorter of two intersecting lines is retained while the longer is discarded until no more lines intersect. An important concept here is the set of conditions that determine whether two *line segments* intersect or not.

In general, the point of intersection of two *lines* y = a_1+b_1x and $y = a_2+b_2x$ is given by $x_i = (a_1 - a_2)/(b_1 - b_2)$ and $y_i = a_1+b_1x_i$. This is just a representation of the intersection point between two lines of infinite length passing through each pair of points. In order to establish that the intersection point lies between the pairs of points (x_1, y_1) and (x_2, y_2) for line segment 1 and, (u_1, v_1) and (u_2, v_2) for the line segment 2, they must satisfy all of the following conditions:

$$\begin{aligned} (x_1 - x_i)(x_i - x_2) &\geq 0 \\ (u_1 - x_i)(x_i - u_2) &\geq 0 \\ (y_1 - y_i)(y_i - y_2) &\geq 0 \\ (v_1 - y_i)(y_i - v_2) &\geq 0 \end{aligned} \tag{2.15}$$

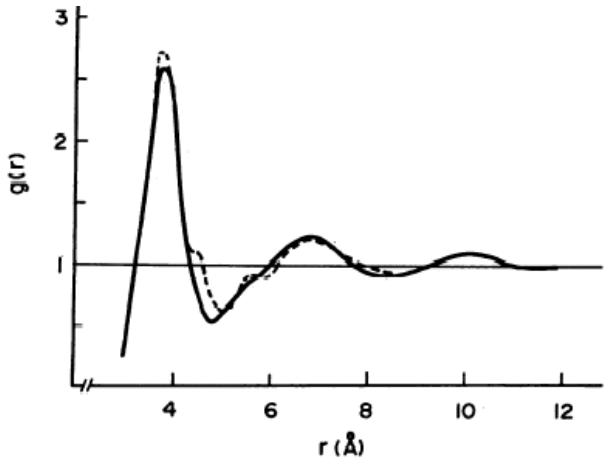

Figure 2.2. Radial distribution function for liquid argon showing typical liquid like structure.

2.5 Radial distribution function

The radial distribution function *g(r)* is an important tool in evaluating the structure of deposited monolayers of colloidal particles. The particle distribution functions measure the extent to which the structure deviates from complete randomness. An important example is structure in liquids because they show no ordering at all. We expect the diffusion-limited deposition structures formed in our research to show the same *g(r)* nature as that of a liquid. A liquid will show a *g(r)* similar to the one represented in Figure 2.2.

From a knowledge of *g(r)* one may try to infer the coordination number N_c (the number of nearest neighbors) of a given particle. The particle coordination number can be obtained by integrating the *g(r)* over a circular area of radius R_c (for two dimensional analysis) and dividing by area per particle *N/A*.

$$N_c = \frac{N}{A}\pi \int_0^{R_c} g(r) r dr \qquad (2.16)$$

If R_c is set at the location of the first peak, the value of *g(r)* at R_c is proportional to the particle coordination number N_c. We therefore do not need to perform the integration as we get a qualitative description of particle coordination number from the value of *g(r)* at the first peak.[39,40]

2.6 Total internal reflection microscopy (TIRM)

TIRM experiments shown schematically in Figure 2.3 measure the scattering intensities of a particle in an evanescent wave. When an incident ray of light passes through a medium with refractive index higher than that of the medium on the other side of the interface at an angle greater than the critical angle, it undergoes total internal reflection. Although no net energy is transferred to the water under conditions of total internal reflection, an optical disturbance occurs in the water, which takes the form of an evanescent wave. Depending on the balance of attractive and the repulsive forces (electrostatic or steric), the particle will sample heights about an equilibrium value by Brownian motion.

The sampling of elevations follows Boltzmann's equation:

$$p(l) = A\exp\left[\frac{-\phi(l)}{kT}\right] \tag{2.17}$$

where *p(l)dl* is the probability of finding the sphere between *l* and *l+dl*, $\phi(l)$ is the potential energy of the sphere at elevation *l*, *kT* is the thermal energy and *A* is a normalization constant whose value is chosen such that $\int p(l)dl=1$.

The particle scatters the evanescent wave at intensities that are dependent on its elevation. A raw data from the experiments is a recording of intensities. The intensity of the evanescent wave decays is the following way:

$$I(l,t) = I_0\exp\left[-\beta l(t)\right] \tag{2.18}$$

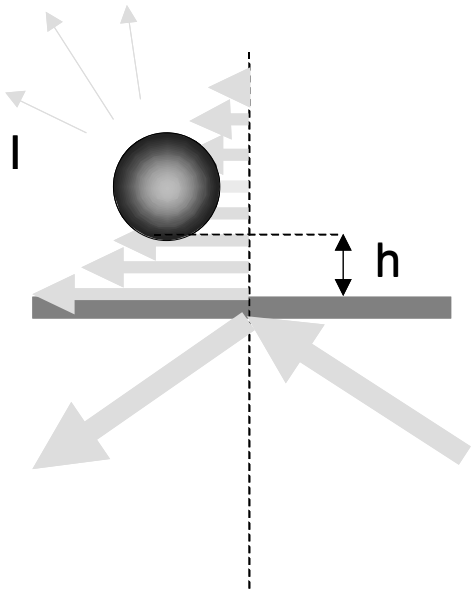

Figure 2.3. Schematic diagram showing particle scattering evanescent wave in TIRM.

where $I(l,t)$ is the scattered intensity at height l and time t, I_o is the minimum scattered intensity and β is the decay length of the evanescent wave (113.67nm for a 633nm He-Ne laser and 97.63nm for a 543nm He-Ne laser). This equation is used to generate a histogram of heights from which the interaction potential is obtained by using Boltzmann's equation.[34]

3. EXPERIMENTAL

3.1 Stamp fabrication and microcontact printing

Polydimethyl siloxane (PDMS, Sylgard 184, Dow Corning) planar stamps are fabricated by pouring a thoroughly mixed 10:1(w/w) mixture of the silicone elastomer and elastomer-curing agent into a petri dish. The size of the petri dish is optional as the stamp is finally cut to the desired size. To ensure good mixing of the elastomer and curing agent, the two are first weighed and mixed in the petri dish for about a minute.[19]

The petri dish is placed in a vacuum chamber for about 3 hours. The dish is then removed form the chamber and placed in an oven set at around 50^{o}C for about 8 hours. The dish removed and allowed to cool. The contents are completely cured by this time and the stamp is then cut out from the dish with a knife. The size of the stamp is kept roughly equal to the diameter of the spin coater stage to be used later.

Silanes are used to modify the properties of glass. This research looks at the modification of glass coverslips using octadecyltrichlorosilane (OTS). Microcontact printing is the preferred method of deposition of monolayer films of OTS on glass because they form better quality films in a much lesser amount of time than films formed by immersion in OTS solutions. The OTS solutions used were prepared by mixing 21μL OTS in 5000μL toluene. This results in a 10mM OTS solution.[24]

Contact printed OTS films are obtained by spin casting the OTS solution onto the PDMS stamp using a conventional photoresist spinner. The spinner is used to apply the solution uniformly without the risk of contaminating the surface with particles. The wetted PDMS stamp is then dried with a stream of nitrogen for 30s, after which it is brought into contact with the substrate (20mm x 20mm zinc titania glass cover slips (SiO_2 64%, B_2O_3 9%, ZnO 7%, K_2O 7%, Na_2O 7%, TiO_2 3%, Al_2O_3 3%)(Corning)) for 30s.[24]

The cover slips used as substrates in the microcontact printing procedure are cleaned by immersing them in a NOCHORMIX solution overnight followed by a

thorough rinsing with deionized water. The coverslips are dried in a stream of nitrogen.

3.2 Polystyrene (PS) spin coating

Clean glass slides (treated with NOCHORMIX) are coated with PS to change their surface properties. The PS solution for spin coating is a 10% (w/w) mixture of PS crystals (Aldrich) in toluene (Fisher Scientific). The mixture is sonicated for around 5 h to ensure complete dissolution of PS. The glass slide is then spun at 1000rpm for 50s with the PS solution. The spin-coated surface is then annealed at 120^{o}C for about 16 hours after which it is slowly brought to room temperature.[29]

3.3 Cell preparation

There are two different types of cells used in this research. The first is prepared using a 1mm x 10mm (*h x id*) O-ring while the second uses a piece of *VWRBRAND* 5/16-inch i.d pipe. Whatever the substrate, the procedure followed for cell preparation is the same.

The O-ring or pipe piece is glued to the substrate with PDMS (Sylgard 184, Dow Corning). After this the samples are allowed to cure overnight (16 hours). Care must be taken to apply PDMS in small amounts to the outside of the O-rings / pipe pieces only. Use of too much PDMS causes spreading onto the area inside the O-ring, which is undesirable.

3.4 Polymer adsorption

The adsorbed polymer used in the experiments is F108 Pluronic triblock copolymer (poly (ethylene oxide)-poly (propylene oxide)-poly (ethylene oxide), or PEO-PPO-PEO) supplied by BASF. Pluronic is adsorbed onto the 4.9 μm surfactant free white sulfate latex colloids (C.V. 4.2%) (Interfacial Dynamics Corporation) by placing them in a shaker with a 1000-ppm polymer solution for 16 h. F108 Pluronic is adsorbed to the substrate surface by allowing approximately 85μL of the 1000ppm Pluronic solution to rest on the substrate surface for 16 h.

3.5 Confocal experiments

A Ziess confocal scanning laser microscope is used to image the first layer of all the deposited structures. The microscope is operated in reflection mode using a 633 nm He-Ne laser. The pinhole is always kept at 1 airy unit. Images are taken at zoom values of 0.7 (pixel/μm = 0.4), 1(pixel/μm = 0.29), 1.7(pixel/μm = 0.17) and 2.7(pixel/μm = 0.11).

The first set of experiments involved the deposition of 2.34 μm silica particles (C.V. 9.9%)(Bangs Laboratories. Inc.) on bare silica surfaces at salt concentrations (NaCl, Aldrich) of 0mM, 5mM, 10mM and 100mM. The solutions used for these deposition experiments were prepared by dispersing 10μL silica sample in 100μL water of desired ionic strength. The resultant solution gives a greater than monolayer surface coverage.

The second set of experiments involved the deposition of 1.0 μm surfactant free white amidine latex colloids (C.V. 4.3%) (Interfacial Dynamics Corporation) on bare silica surfaces in deionized water. The concentrations in this case were chosen so that monolayer surface coverage was achieved.

The third set of experiments involved the deposition of 2.34 μm silica particles (C.V. 9.9%)(Bangs Laboratories. Inc.) on bare silica surfaces at a salt concentration (NaCl, Aldrich) of 10mM and pH values of 5.5 and 10mM. The solutions used for these deposition experiments were prepared by dispersing 10μL silica sample in 100μL water of desired ionic strength. The resultant solution gives a greater than monolayer surface coverage. The fourth set of experiments involved deposition experiments involving polymer (F108 Pluronic, BASF) coated 4.9 μm surfactant free white sulfate latex colloids (C.V. 4.2%) (Interfacial Dynamics Corporation) at various salt concentrations.

The analysis of the images was done in two steps. The first involved obtaining particle coordinates. A two-dimensional center program was used for this purpose. The next step involved the determination of fractal dimension. A Fortran program described

in the theory section was used for this purpose. Other programs like triangulation, bond orientation order and radial distribution function were also run.

3.6 TIRM experiments

The first step in setting up the TIRM experiment involves the cleaning of the prism (Reynard Corporation) with acetone (purchased from Fisher Scientific and used without further purification). Polymer solution is drawn off the substrate (cell) to be studied. A drop of index matching oil (refractive index = 1.516±0.0002 purchased from SPI supplies) is placed on the cleaned prism and the cell is carefully lowered onto the drop in order minimize the trapping of air bubbles beneath the cell. Approximately 85μL of polymer coated PS particles in desired solvent is introduced into the cell. The cell is closed off form above by a glass slide to minimize evaporation.

The prism is placed on the microscope stage and is allowed to stand for 15min. This allows enough time for the PS particles to sediment. A Hamamatsu *ORCA-ER* C.C.D. camera is used to capture images of the particles over the surface. The particle scatters an evanescent wave produced by total internal refection of a 543 nm He-Ne laser. The solutions of 0.5M concentrations were prepared by diluting the original polymer coated solution of PS spheres with a 1M NaCl solution.

For each analysis, 90000 frames were captured. The raw data form the experiment is in the form of an intensity distribution. Equation (2.18) is used to convert the intensity distribution into a histogram of heights. Particle-wall potential is obtained by using the histogram of heights and the Boltzmann equation given by Eq. (2.17). We used image analysis codes available in the group to perform the above mentioned data manipulations.

4. DIFFUSION LIMITED DEPOSITION

4.1 Introduction

This part of the research deals with a specific class of colloidal interaction. As stated earlier, an investigation into particle-particle and particle-surface interactions helps in determining the equilibrium configuration or the most thermodynamically favored state. Kinetically trapped states formed in systems of hard spheres on the earth's surface are not observed in space.[41] An in-depth understanding of interactions that result in the occurrence of such states needs to be done. Colloidal systems in which strong attractive interactions predominate are one such example. Such systems always undergo diffusion-limited deposition.

Diffusion limited deposition can be easily explained by looking at rapidly aggregating systems.[17] Diffusion limited colloidal aggregation occurs when there is a negligible repulsive force between colloidal particles, so that the aggregation rate is limited solely by the time taken by particles to encounter each other by diffusion. The particles stick to each other before they have sufficient time to rearrange and this results in the formation of disordered solid aggregates. Past studies have evaluated the structures of diffusion limited colloidal aggregates by way of fractal theory.[16,42]

The low fractal dimension of aggregates reflects their open structure.[1,43] The most important finding of these studies is that for any system of colloids in which the predominant inter-particle force is a large attraction; (either electrostatic, van der Waals, or polymeric) the resulting structures all have approximately the same value of fractal dimension (1.44 ± 0.04).[1,2]

This research characterizes the fractal dimension of structures formed on surfaces by deposition in the diffusion-limited regime. As a preliminary check for the fractal dimension program used, fractal dimensions of simulated clusters (in diffusion controlled regime) are evaluated and checked against typical values for diffusion limited colloidal aggregates listed in the literature.[1,2,43] Images obtained using CLSM allow

surface structures generated via diffusion-limited deposition to be characterized. Fractal dimension, radial distribution, bond orientational order parameter and triangulation methods are used to characterize the amount of order in the images.

Two different colloidal systems, both under diffusion-limited conditions, are investigated. The first is a system of silica particles deposited on a silica surface at a very large salt concentration (100mM) (resulting in complete screening of electrostatics). The only inter-particle and particle-wall force acting on this system apart from hydrodynamics and the external gravity field is van der Waals attraction. The second system involves the deposition of positively charged latex spheres on a negatively charged silica surface. The predominant attractive interaction in this experiment is electrostatic.

4.2 Theory

4.2.1 Fractal dimension: evaluation and interpretation

As discussed in the theory, sets of points that have non-integer dimensions or a "fraction of a dimension" and are called fractals.[37] To analyze the fractal dimension of any cluster of colloids, a general Fortran code has been written, tested, and employed specifically in this work to analyze confocal images of surface structures generated via diffusion limited deposition. The program uses a cluster sorting code to isolate clusters of particles and then finds the fractal dimension for each cluster. The Fortran code uses Eq.(2.8-2.10) to evaluate fractal dimension of clusters.

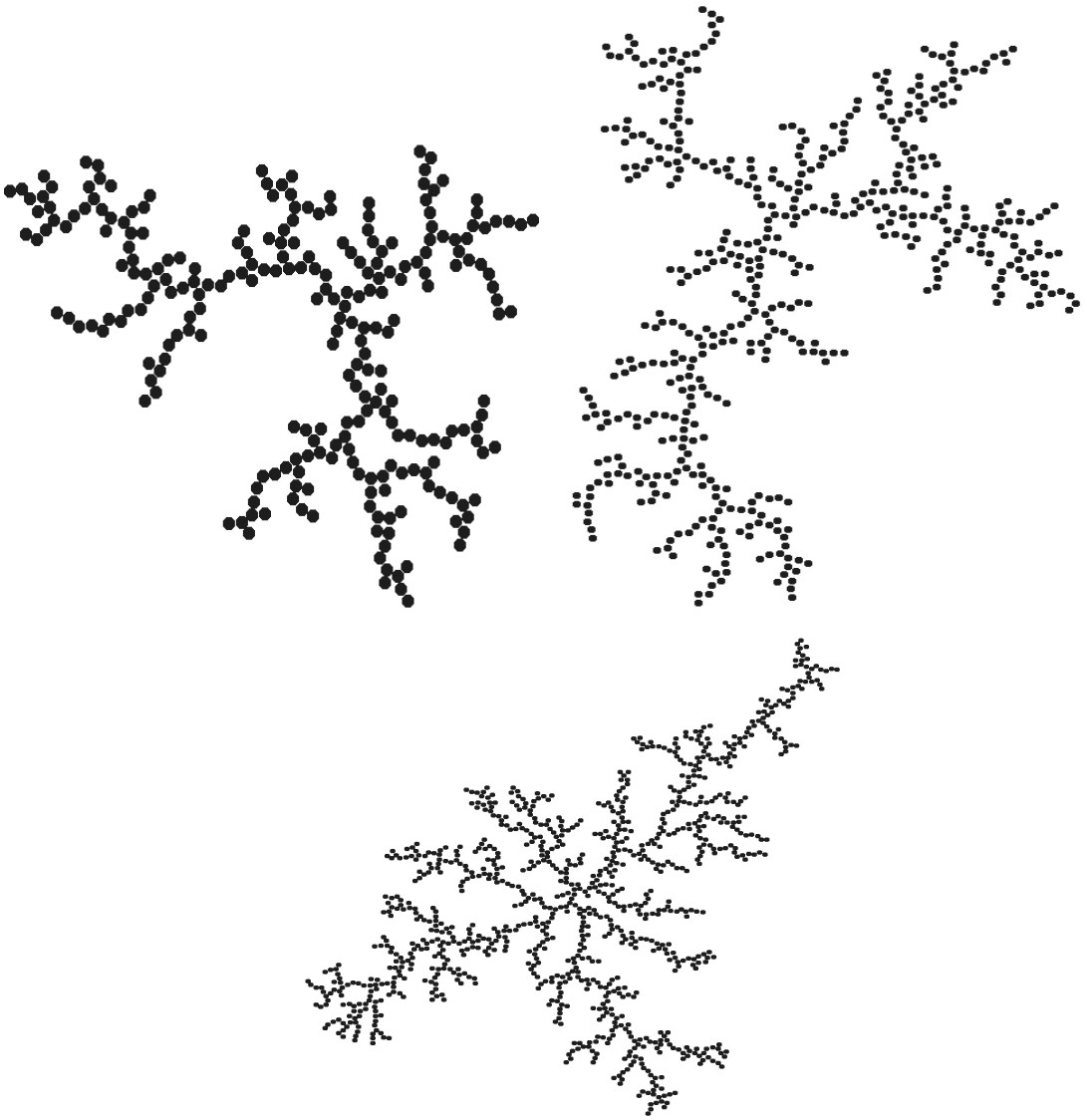

Figure 4.1. Sample images of diffusion limited aggregates of (L-R) 256, 512 & 1024 particles respectively used for verification of the fractal dimension program.

To verify the effectiveness of this program, we tested it for sample images formed from diffusion-limited kinetics. It is already known from literature that for two-dimensional clusters formed by diffusion-limited kinetics, the value of fractal dimension is around 1.44 ± 0.04.[2-4] The images of the particles are in Figure 4.1. The value of fractal dimension obtained after running the fractal dimension program on the three

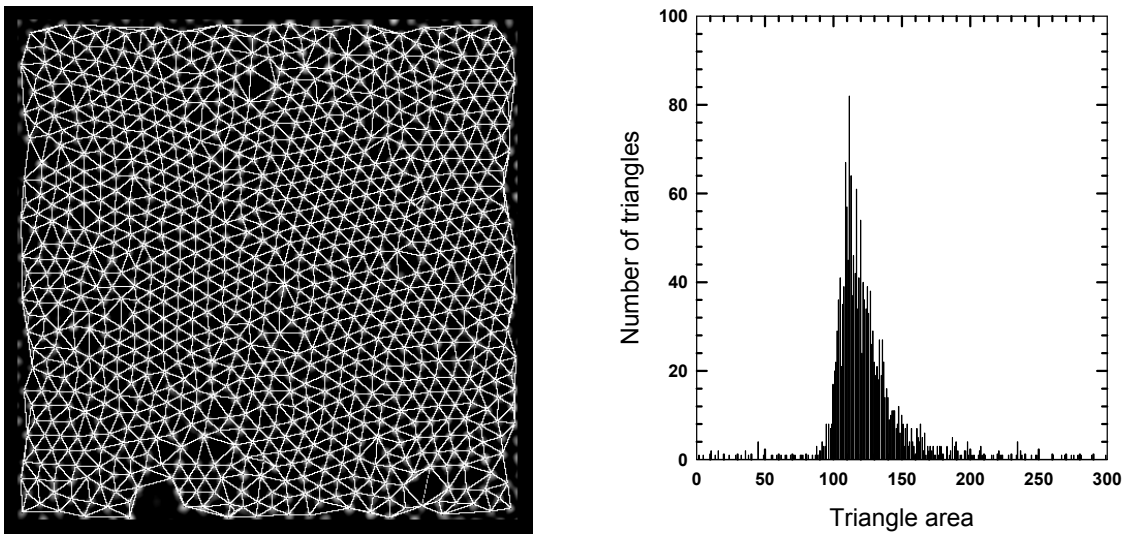

Figure 4.2. Triangulation (Image and histogram) for 2.34μm silica spheres on silica surface at 5mM NaCl.

sample images is shown in Table 4.1. The error is evaluated against the mean value of 1.44 in each case. The fractal dimensions shown by the program for all the cluster sizes are quite accurate but it is easy to see that the results are much more accurate for clusters with higher numbers of particles. Since most of the images we will be evaluating have between 900 and 1200 particles we can confidently state that our program functions very accurately in this range.

Table 4.1 Performance of the Fortran fractal program

Number of Particles	Fractal dimension given by program	% Error
256	1.54	6.94
512	1.49	3.47
1024	1.44	0

4.2.2 Bond orientational order parameter, radial distribution function and triangulation

These are the other methods used to characterize the amount of order in the confocal images. Fortran codes available in the research group are modified and used

for this purpose. Global bond orientational order parameter (Ψ_X) is a single parameter useful for characterizing two-dimensional order. X is an integer related to the coherence of X-fold symmetry (X = 6 for hexagonal 6-fold symmetry and X = 4 for square 4-fold symmetry). Regardless of the symmetry type, Ψ_X approaches 1 for perfect order or a number approaching zero for random configurations.[44] Local bond orientational order parameter is another important indicator of structure quality but is not used in this study.

$$\psi_X = \left| \frac{1}{N} \sum_j \sum_k e^{Xi\theta_{jk}} \right| \tag{4.1}$$

The triangulation program draws lines between every particle center in the image. The shorter of two intersecting lines is retained while the longer is discarded according to Eq.(2.15) until no more lines are intersecting. The program then generates a histogram of triangle area for the image. For perfect two-dimensional order, there will be only one sharp peak in the histogram, as all triangles will have the same area. For disordered structures, the peak is flatter as shown in Figure 4.2. The program used has a few unresolved flaws but does a relatively good job of representing the amount of order in the system.

4.2.3 Fuchs stability ratio

Fuchs stability ratio will be used in this research section to verify the existence of diffusion-limited kinetics. A MathCAD document was written for this purpose. To validate the MathCAD worksheet, we first reproduced a plot of stability ratio at high ionic strengths against particle size for polystyrene particles from Russel et al. (Page 276).[8] The potentials and hydrodynamic interactions used are for particle-particle PS systems Eq.(2.3). The plot is shown in Figure 4.3. The MathCAD worksheet was then used to predict the onset of diffusion-limited kinetics in systems with silica particle-silica surface interactions. The worksheet used Eq.(2.11, 2.12, 2.14). The onset of diffusion-limited kinetics is seen in Figure 4.4 to be at approximately 91.6mM. The experiment conducted at 100mM therefore corresponds to diffusion-limited deposition.

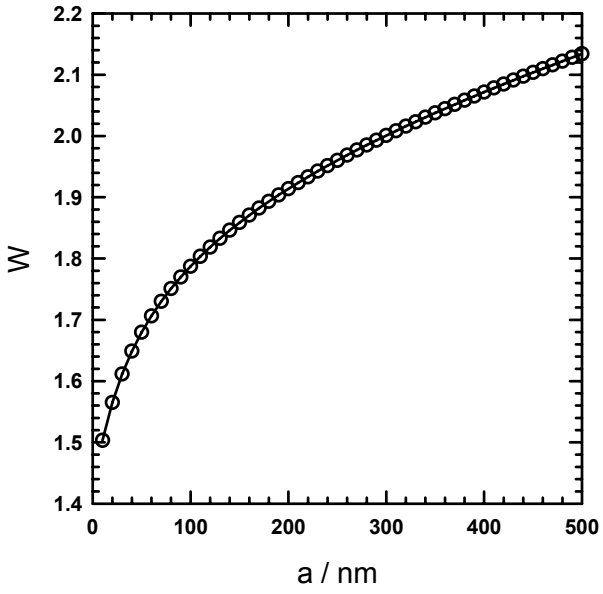

Figure 4.3. Fuchs Stability Ratio for rapid flocculation of PS lattices in water as a function of sphere radius generated by use of MathCAD worksheet and equations (2.3, 2.11, 2.13).

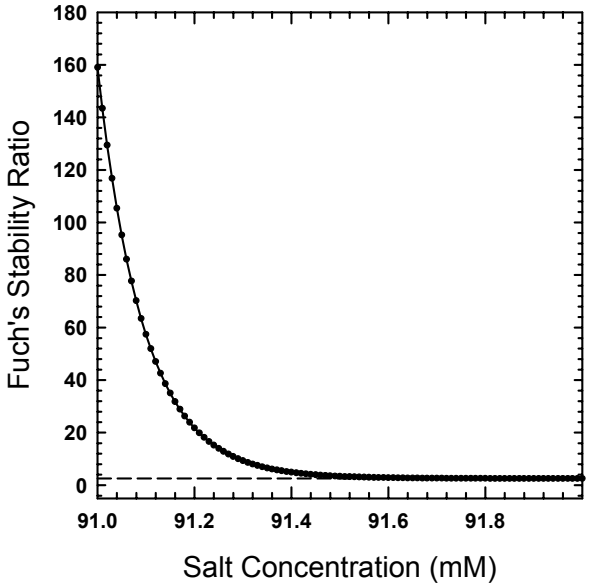

Figure 4.4. The onset of diffusion-limited kinetics for a system with 2.34μm silica spheres interacting with silica substrate generated using MathCAD spreadsheet and equations (2.11, 2.12, 2.14).

4.3 Experimental

4.3.1 Materials

2.34μm silica colloids (C.V. 9.9%)(Bangs Laboratories. Inc.) and 1.0μm surfactant free white amidine latex colloids (C.V. 4.3%) (Interfacial Dynamics Corporation) were used in the experiments. Sodium chloride (NaCl), used to control the ionic strength in these experiments was purchased from Aldrich and used without purification. 20mm x 20mm zinc titania glass cover slips (SiO_2 64%, B_2O_3 9%, ZnO 7%, K_2O 7%, Na_2O 7%, TiO_2 3%, Al_2O_3 3%)(Corning) were used as substrates in the deposition experiments.

4.3.2 Cell preparation

The colloidal deposition was carried out in sedimentation cells. The cells used for the deposition experiments involving the silica particles were constructed by attaching 1mm x 10mm (*h x id*) O-rings to 20mm x 20mm cover slips (Corning) using polydimethyl siloxane (PDMS, Sylgard 184, Dow Corning). The cells used for the deposition experiments involving amidine particles were constructed by attaching cut pieces of *VWRBRAND* 5/16-inch i.d pipe to 20mm x 20mm cover slips (Corning) using polydimethyl siloxane (PDMS, Sylgard 184, Dow Corning). The sedimentation cells were always covered with another 20mm x 20mm cover slip to avoid evaporation. Vacuum grease was used to seal the top cover slip onto the O-ring or pipe piece.

The dispersions of silica colloids were prepared by mixing 25 μL of 9.9% (v/v) silica colloids with 250 μL water with a required amount of NaCl. The dispersions of amidine particles used had concentrations that would give monolayer coverage. The cover slips were cleaned by immersing them in Nochromix overnight and then washing them repeatedly in de-ionized water. The cover slips were dried in a stream of nitrogen gas.

4.3.3 Confocal imaging

A Ziess confocal scanning laser microscope was used to image the first layer of all the deposited structures. The microscope was operated in reflection mode using a 633 nm He-Ne laser. The pinhole was always kept at 1 airy unit. Images are taken at zoom values of 0.7 (pixel/μm = 0.4), 1(pixel/μm = 0.29), 1.7(pixel/μm = 0.17) and 2.7(pixel/μm = 0.11).

4.3.4 Procedure

The first experiment involved varying the ionic strength of the solution of silica particles and observing the structures formed. Images of the first layer of silica particles were recorded for 0mM, 1mM, 5mM, 10mM and 100mM NaCl concentrations. The second experiment involved the deposition of amidine-latex particles on the cover slips. This experiment was performed for particles in de-ionized water.

4.4 Results and discussion

4.4.1 Surface structure in silica particles on glass as a function of ionic strength

For all images captured, fractal dimension and bond-orientation order parameter were determined. The radial distribution function and triangulation analyses were also performed for all the data recorded. The structure of the surface layer of colloids becomes less ordered with increasing salt concentration. This is clearly revealed by the values reported in Table 4.2 and Figure 4.5.

Table 4.2 Effect of ionic strength on structure of deposited colloidal layers

Salt Concentration (mM)	Debye Length (nm)	Fractal Dimension	Ψ_6	Ψ_4
0 mM	303.16	1.885	0.936	0.083
5 mM	4.28	1.834	0.290	0.062
10 mM	3.03	1.808	0.045	0.039
100 mM	0.96	1.725	0.031	0.056

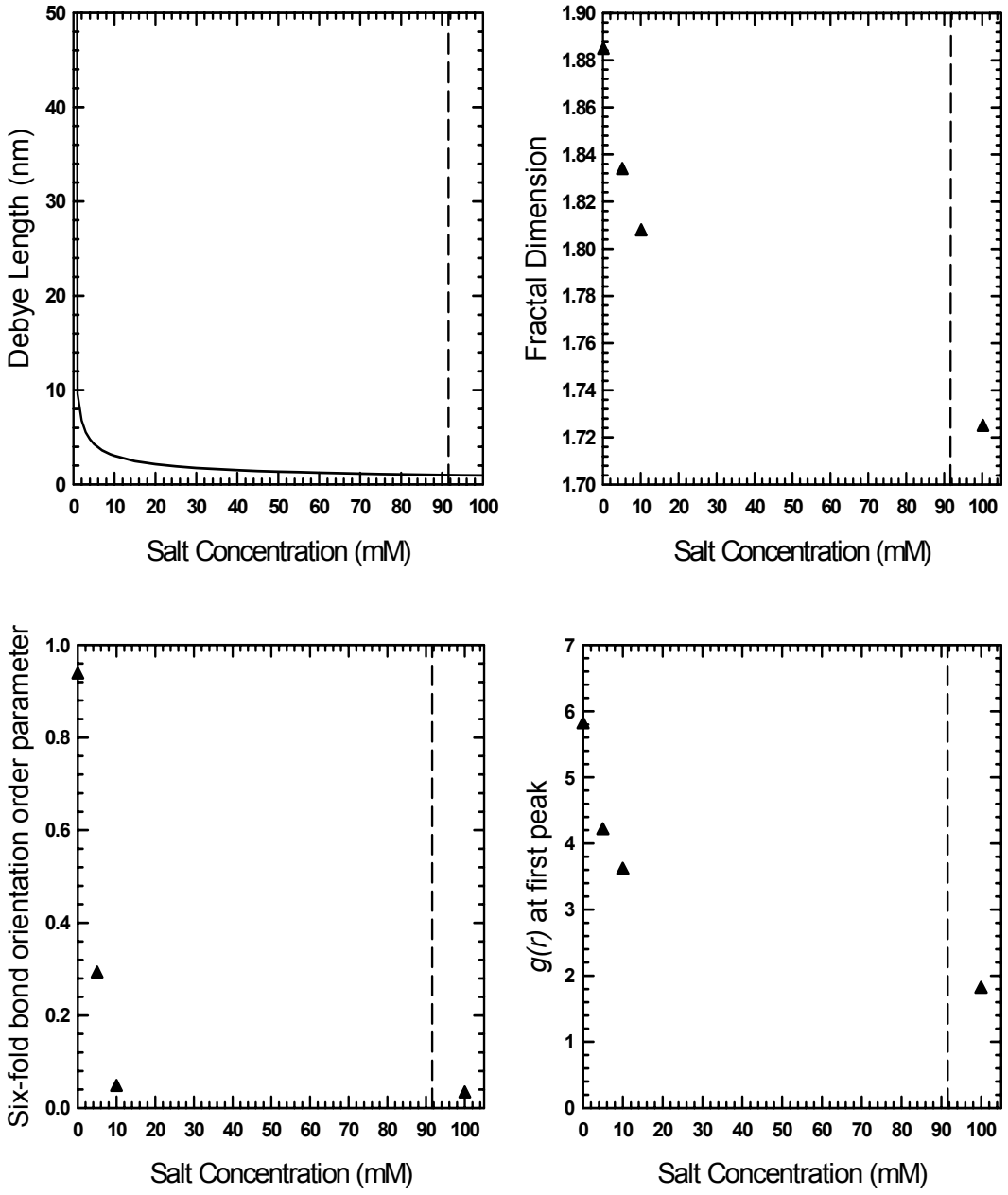

Figure 4.5. Influence of rapid deposition kinetics on the structural characteristics of 2.34μm deposited silica particles. The line at 91.6Mm in each plot shows the onset of diffusion-limited kinetics as predicted by Fuchs stability ratio.

As the ionic strength of the solution is increased, the electrostatic forces, which help to keep the particles apart, diminish. The Debye length reduces and the particles

have less space to move and less time to rearrange due to reduced diffusion coefficient via many-body hydrodynamic interactions with neighboring particles. At 100mM, the electrostatics is completely screened and the only interaction in the system is van der Waals attraction. Diffusion limited deposition occurs, resulting in a structure with lesser order. The Fuchs stability ratio confirms that 100mM salt concentration corresponds to diffusion-limited case.

The system stability ratio is first determined for the case where the interaction potential only contains van der Waals attraction (W_∞) (electrostatics is completely absent/high salt concentrations). This corresponds to the diffusion-limited regime. The stability ratio is then worked out for the actual interaction potential in the system, which depends on the salt concentration (W). A ratio of these two quantities (W/W_∞) is plotted against salt concentration (mM). The point where the curve levels out to 1 represents the onset of diffusion limited kinetics. It is clear from Figure 4.4 that 91.6mM is approximately where this onset occurs.

The radial distribution functions as well as the triangulation histograms are obtained for each image recorded. While the radial distribution function for the 0mM case clearly shows crystalline structure, the degree of ordering is destroyed as the salt concentration is increased to 100mM. An important point to be noted here is that the crystal structure formed at 0 salt concentrations is purely repulsive and hence very week. The structure formed at 100mM is stronger on account of the predominance of attraction but also very disordered on account of the high degree of attraction as seen in Figure 4.6. The particle co-ordination number, which is related to the value of *g(r)* at the first peak shows a drastic change as the ionic strength is increased as shown in Table 4.3. At low ionic strengths the value of *g(r)* at the first peak is almost 6 that represents an almost perfect crystal. At 100mM salt concentration that corresponds to diffusion-limited kinetics, the value of *g(r)* at first peak is barely 2.

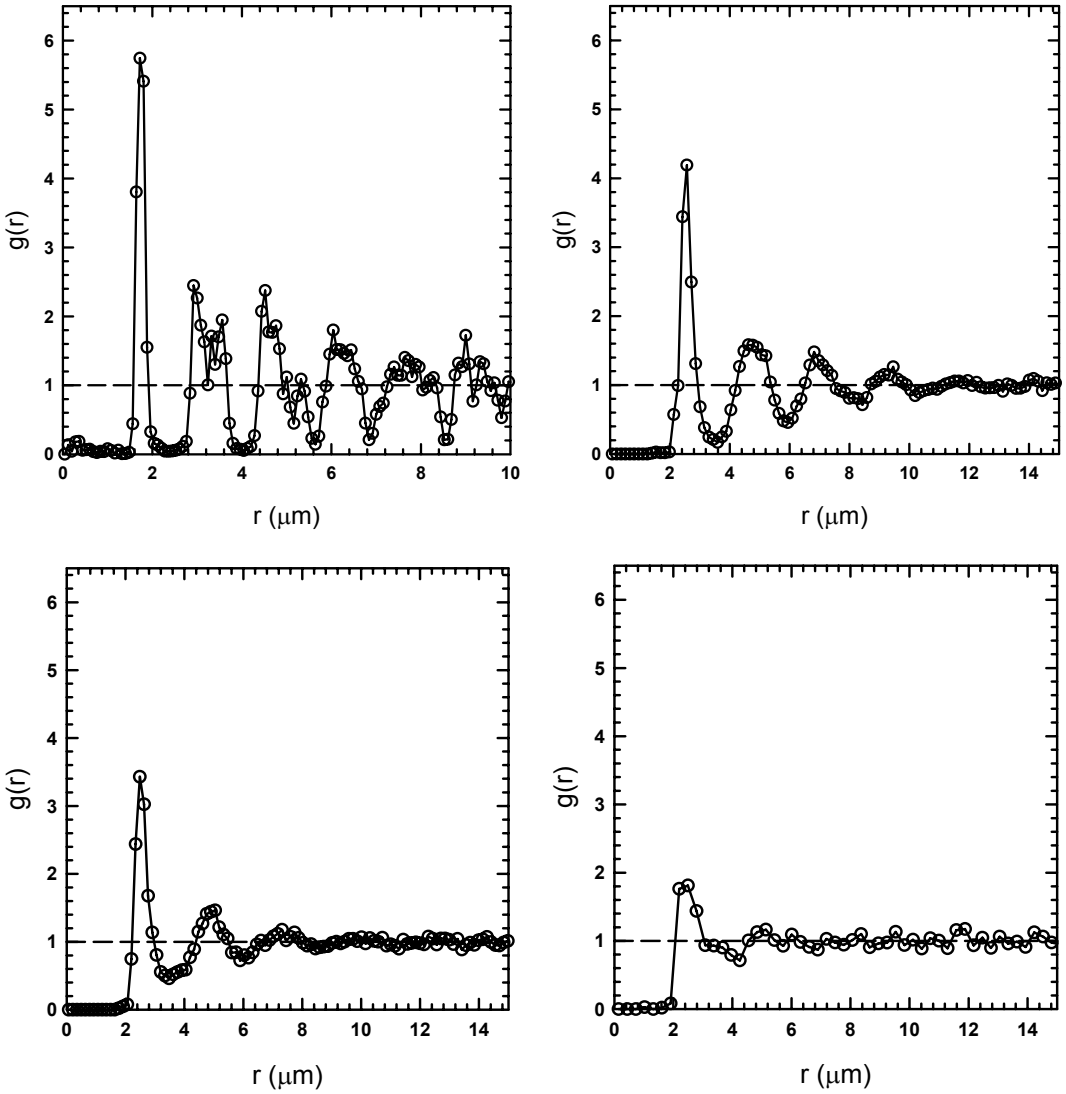

Figure 4.6. Radial distribution functions for 2.34μm silica particles on silica substrate at (L-R): 0mM, 5mM, 10mM, and 100mM salt concentrations respectively.

Table 4.3 Deviation from crystallinity with increase in ionic strength

Salt Concentration (mM)	*g(r)* at first peak
0 mM	5.8
5 mM	4.2
10 mM	3.6
100 mM	1.8

The triangulation histograms show a broadening of the peak as the salt concentration is increased. This also indicates the diminishing order in the system. The results for the triangulation histograms are in Figure 4.7. All the analyses show that for systems in which the only interaction is van der Waals attraction, structures with lesser amounts of order form.

Large single domain crystalline colloidal structures are easily assembled under low salt concentrations. The main cause is the electrostatic repulsion, which keeps the colloids separated from each other. The repulsion allows the particles greater space and time to diffuse around and adopt the lowest free energy configuration, which is the ordered state. As the salt concentration is increased, the repulsive force diminishes and the particles sit at closer separations, which results in them having a reduced freedom of movement. At salt concentrations where the only interaction is attractive, the particles have no time to adopt the lowest free energy configuration. This is easily seen in Table 4.2 and Figure 4.5 where the Debye length decreases rapidly with increasing ionic strength. At low ionic concentrations, the large Debye lengths mean that the electrostatic repulsion ensures a large average interparticle separation. The crystalline structures formed at low ionic strengths are not robust.

At high salt concentrations, the predominance of attraction results in the formation of disordered structures. The study was conducted for two different types of attractive interactions. The observations from the first experiment with the silica particles show that strong attraction leads to the formation of disordered structures. The predominant interparticle and particle substrate interaction in this set of experiments was van der Waals attraction. The Fuchs stability ratio calculation shows that the images analyzed for the 100mM salt concentration case correspond to structures formed by diffusion-limited kinetics. As expected the lack of time for particle rearrangement leads to the formation of random structures.

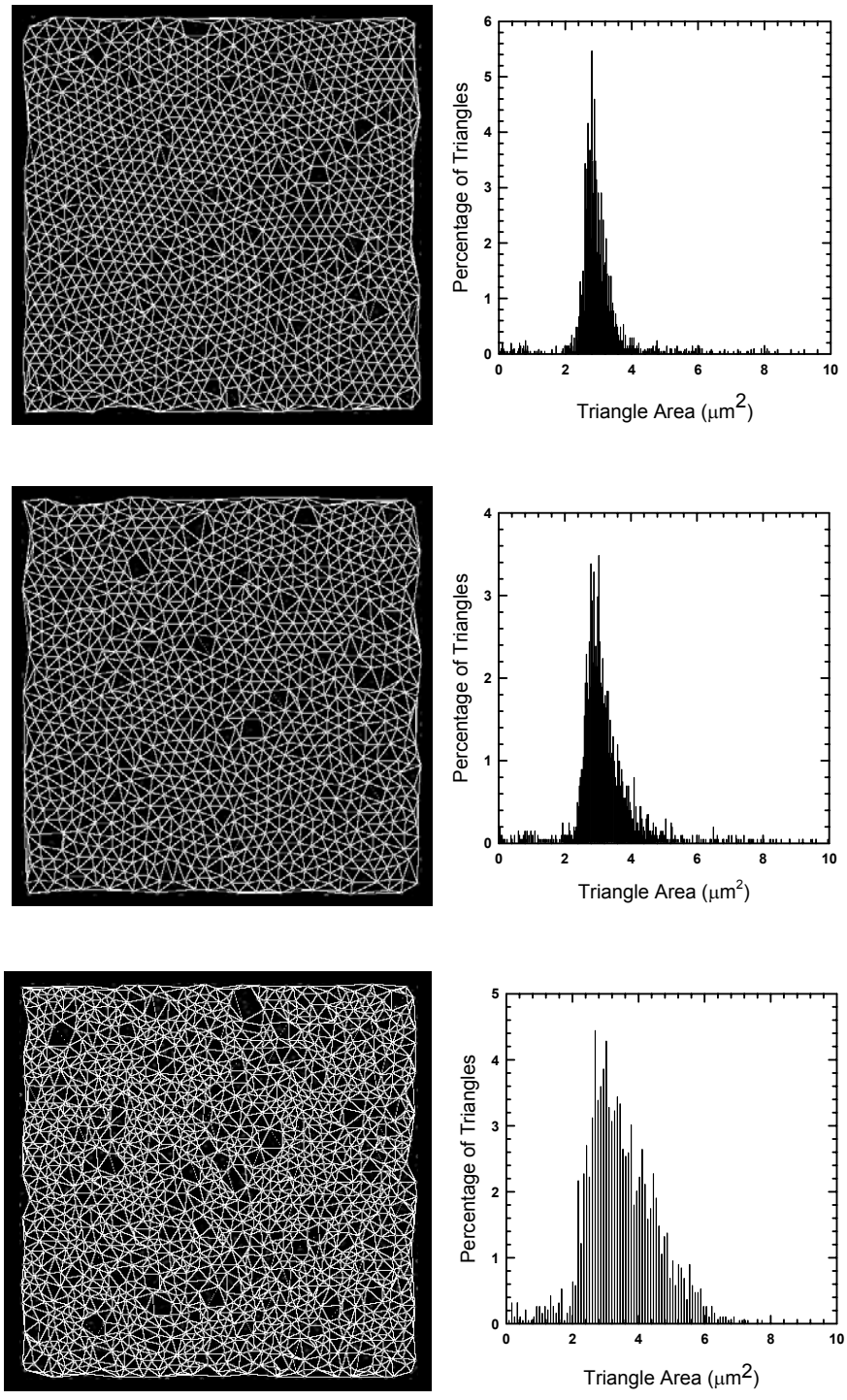

Figure 4.7. Triangulation histograms for a system of 2.34μm silica particles on silica substrate at 5mM, 10mM and 100mM salt concentrations respectively.

4.4.2 Surface structure in amidine terminated latex particles on glass

The next experiment involved another system in the diffusion-limited regime. The difference was that the predominant attractive interaction was electrostatic. The other important difference was that this experiment was performed at monolayer surface coverage unlike the earlier experiments with the silica particles. The system shows a fractal dimension value of about 1.462. Also of importance are the bond orientational order parameter, radial distribution function, and triangulation analyses, all of which indicate a highly disordered structure. The radial distribution function shows a typical profile for a disordered structure with a low first peak value of *g(r)* at 1.4 as compared to 6 for perfect order. (See Table 4.4 and Figure 4.8)

To understand the effect of the nature of attractive interaction in this kinetic regime, it was essential to perform an experiment on a system that was governed by similar kinetics but had a different attractive force. The experiments with the amidine-latex particles deposited on the glass cover slips were performed for this purpose. The predominant particle-substrate force in this case was the electrostatic attraction between the positively charged amidine spheres and the negatively charged glass. The results show that for any system undergoing diffusion limited deposition, the nature of the structures formed was the same.

Table 4.4 Poor ordering due to large electrostatic attraction

Type of System	**Predominant attractive interaction**	**Fractal Dimension**	**Ψ_6**	**Ψ_4**
Amidine terminated (positively charged) spheres deposited on glass in deionized water	Electrostatic	1.462	0.016	0.014

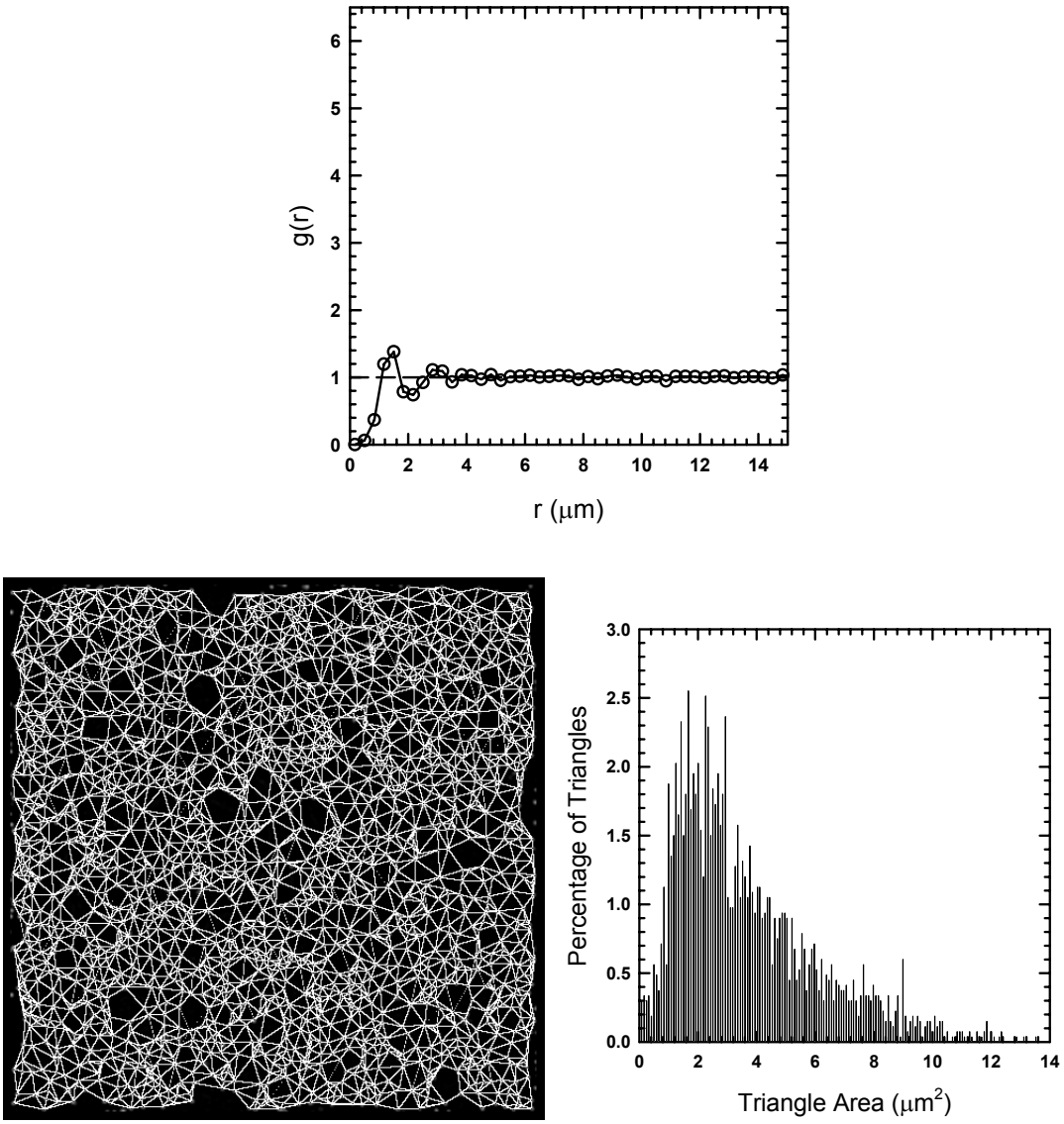

Figure 4.8. Radial distribution functions and triangulation analysis for diffusion limited deposition of positively charged 1μm amidine terminated latex colloids on negative glass surface.

The bond orientational order parameters for both cases are almost zero. The radial distribution functions have almost the same nature. Figure 4.9 shows a plot of radial distribution functions for both systems. The closed dots represent the amidine system while the open dots represent the silica system. The low first peak *g(r)*, 1.8 for

silica particles in 100mM solvent and 1.4 for amidine terminated latex spheres in deionized water) in both systems indicates random structures.

Flat peaks in the triangulation histograms for both cases reveal a lack of order in systems with attraction as the predominant interaction. The only difference between the two systems, apart form the nature of the attractive force, was the concentrations used. The amidine experiments were performed at monolayer concentrations while the silica experiments were conducted at much higher concentrations. This is clearly evident in the values for fractal dimensions in the systems. Pressure from the upper layers cause the silica particles in 100mM solvent to pack more tightly (but randomly) on the glass surface resulting in a noticeably higher value of fractal dimension. The amidine particles are not under any such pressure and adopt a more open structure. The value of fractal dimension reported in this case (1.462) is very close to the value reported in the literature (1.44 ± 0.04) for aggregating systems in the diffusion-limited regime.

In conclusion, once the predominant particle-particle and particle-substrate interaction is strongly attractive, the nature of the attractive interaction is not important in determining the final structure. It also reveals that large attractive interactions are not favorable for producing long-range order.

4.5 Conclusions

This research section shows two things. The nature of the attractive force is immaterial in case of systems undergoing diffusion limited deposition. Large attractive interactions allow no time for particles to diffuse and find the lowest free energy configuration on a substrate. The result is the formation of disordered structures.

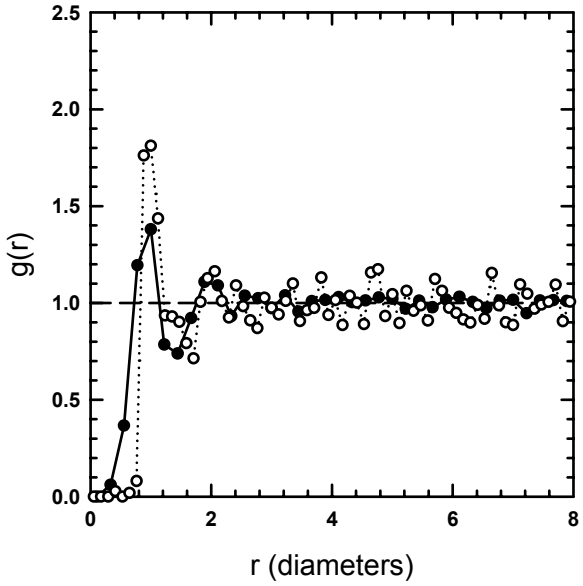

Figure 4.9. Radial distribution functions for diffusion limited deposition of positively charged colloids on glass surface (closed dots, predominant attractive force is electrostatic) and diffusion limited deposition of silica spheres on glass at high ionic strength (open dots, predominant attractive force is van der Waals) where each data set is normalized by the separation at the first peak (particle diameter).

5. REACTION LIMITED DEPOSITION

5.1 Introduction

The research in the previous section clearly indicates that using large attractive interactions results rapid deposition and disordered structures. This section looks at deposition processes in which there is a substantial but not insurmountable repulsive barrier between particles and a homogeneous substrate. The importance of the height of the repulsive barrier is illustrated in Figure 5.1. The black curve is the reaction limited case while the gray curve represents the diffusion limited case. In the reaction-limited case, it will take some time for the particles to obtain sufficient kinetic energy (by Brownian motion and particle-substrate collisions) to overcome the repulsive barrier. In the diffusion limited case however, there is no potential energy barrier to overcome and the particles stick on their fist encounter.

The particles have no time to rearrange in the diffusion-limited case. A barrier height that forces the particles to stay apart sufficiently long such that they have time to rearrange, will lead to more ordered structures.[2-4] The rate of deposition in this case is limited by the time the particles take to overcome the particle-wall repulsive barrier. The settling particles will experience a number of collisions before they have an encounter of enough energy to overcome the energy barrier to produce deposition in the case of particle-wall interactions or aggregation for particle-particle interactions.[1,45]

Reaction limited deposition processes allow a much longer time for rearrangement of particles on the surface of a substrate and therefore result in the formation of more organized and compact structures. The current research section will study reaction-limited colloidal deposition by the use of TIRM and CLSM. Results involve the TIRM analysis of silica particles interacting with a silica surface (glass slide). The previous research section involved deposition of silica colloids on a silica surface. This section studies the same system but the experiments are concentrated on a different set of conditions.

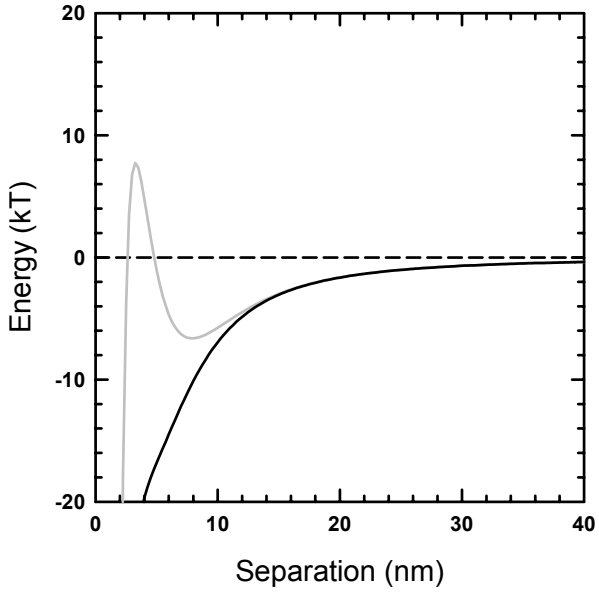

Figure 5.1. Importance of the repulsive energy barrier, a kinetic barrier associated with electrostatics.

TIRM and CLSM analyses will be conducted for two solvent conditions. The experimental conditions in the first run are 10mM salt concentration and pH 5.5(on account of dissolved carbon dioxide in de-ionized water) while the second has 10mM salt and pH 10.

The surface charge of silica almost doubles when the pH is changed form 5.5 to 10. The experiments are setup to study the effect of increasing barrier height on the ordering of particles on the homogeneous substrate. It is important to mention that the purpose of this study is to analyze and understand the reaction-limited regime. A direct requirement of this study is therefore that the repulsive barrier be substantial but not insurmountable. The system is therefore studied at a salt concentration of 10mM as lower salt concentrations result in an insurmountable barrier.

The CLSM experiments make the analysis of reaction-limited kinetics comprehensive. The TIRM experiment allows the measurement of the particle-substrate interaction. The aim in this research section is to show that particles form structures

with a different amount of order in the reaction-limited regime as compared to the diffusion controlled deposition regime. The sub-monolayer-coverage concentrations used in TIRM experiments result in images that show an average of only 6-7 particles per window, which are not enough for performing an evaluation of the structures these systems form. The final experiments in this research section involve the use of CLSM to evaluate the quality of the packing formed by this reaction-limited deposition system.

5.2 Experimental

5.2.1 Materials

2.34μm silica colloids (C.V. 9.9%)(Bangs Laboratories. Inc.) were used in the experiments. Sodium chloride (NaCl), used to control the ionic strength in these experiments was purchased from Aldrich and used without purification. Potassium hydroxide (KOH), used to control the pH in these experiments was purchased form Fisher Scientific and used without purification. 20mm x 20mm zinc titania glass cover slips (SiO_2 64%, B_2O_3 9%, ZnO 7%, K_2O 7%, Na_2O 7%, TiO_2 3%, Al_2O_3 3%)(Corning) were used as substrates in the deposition experiments.

5.2.2 Cell preparation

The colloidal deposition was carried out in sedimentation cells. The cells used for the deposition experiments were constructed by attaching 1mm x 10mm (*h x id*) O-rings to 20mm x 20mm cover slips (Corning) using polydimethyl siloxane (PDMS, Sylgard 184, Dow Corning). The sedimentation cells were always covered with another 20mm x 20mm cover slip to avoid evaporation. Vacuum grease was used to seal the top cover slip onto the O-ring or pipe piece.

The dispersions of silica colloids were prepared by mixing 25 μL of 9.9% (v/v) silica colloids with 250 μL water with a required amount of NaCl. The cover slips were cleaned by immersing them in a Nochormix overnight and then washing them repeatedly in de-ionized water. The cover slips were dried in a stream of nitrogen gas.

The cells used in the TRIM experiments were prepared in exactly the same way as those used for the CLSM studies. Before use in the TIRM experiment, the glass slides were immersed in a 0.1mM KOH solution for about ½ hour to maximize the surface charge of silica. The prism used in the experiment was cleaned with acetone.

5.2.3 Confocal imaging

A Ziess confocal scanning laser microscope was used to image the first layer of all the deposited structures. The microscope was operated in reflection mode using a 633 nm He-Ne laser. The pinhole was always kept at 1 airy unit. Images were taken at various zoom values. Images are taken at zoom values of 0.7 (pixel/μm = 0.4), 1(pixel/μm = 0.29), 1.7(pixel/μm = 0.17) and 2.7(pixel/μm = 0.11).

5.2.4 TIRM analysis

A Hamamatsu *ORCA-ER* C.C.D. camera was used to capture images of the sample over the surface. The particle scatters an evanescent wave produced by total internal refection of a 543 nm He-Ne laser.

5.2.5 Procedure

The CLSM experiments involved varying the pH of the 10mM solution of silica particles and observing the structures formed. Images of the first layer of silica particles were recorded for 10mM NaCl concentration and pH conditions of 5.5 and 10. The TIRM experiment involved the levitation study of the same particles on the cover slips. This experiment was also performed for particles in 10mM NaCl and pH conditions of 5.5 and 10.

5.3 Results and discussion

5.3.1 Measurement of pH dependent deposition and structure on silica substrates (CLSM studies)

By keeping the concentration of particles and the overall system the same, an effective determination of the effect of pH on the order in the deposited layers is possible. For all images captured, fractal dimension and bond-orientational order parameter were determined. The radial distribution function and triangulation analyses were also performed for all the data recorded. The results clearly indicate a higher value of fractal dimension for pH 10 as compared to pH 5.5. The six-fold bond orientation order parameter value shows a jump form almost zero to 0.117. The results discussed in the paragraph are summarized in Table 5.1.

The radial distribution functions as well as the triangulation histograms are obtained for each image recorded. The radial distribution (Figure 5.2) function for the pH 10 case clearly shows a greater degree of ordering than the pH 5.5 case. The value of *g(r)* at the first peak shows a drastic change as the pH is increased (Table 5.1). At pH=5.5 the value of *g(r)* at the first peak is 3.6 while at pH=10 it increases to 3.8. Both experimental conditions correspond to reaction-limited kinetics.

The triangulation histograms give probably the best indication of the increase in the amount of order in the surface layer as the pH is increased. For the same system, just a change in the pH causes the histogram to get less flat. This is clearly seen in Figure 5.3. The triangulation histogram for the 10mM and 5.5-pH case shows a peak width of approximately 3 μm^2 while the triangulation histogram at 10mM and 10-pH shows a peak width of only 1 μm^2. This clearly illustrates that the higher repulsive barrier leads to greater degrees of ordering. The triangulation results are summarized in Figure 5.3.

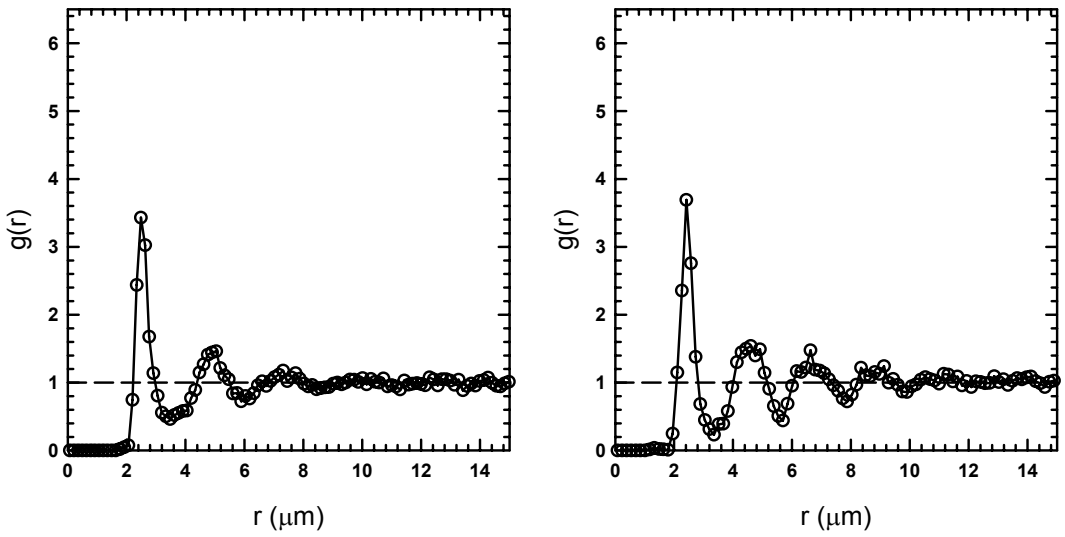

Figure 5.2. (L-R) Radial distribution functions for pH =5.5 and pH =10. (Bottom) Comparison of radial distribution functions clearly showing greater ordering at pH = 10 (Closed dots) than at
pH = 5.5 (Open dots).

Table 5.1 Change of solvent conditions in reaction-limited regime to achieve higher amounts of order

Salt Concentration (mM)	pH	Fractal Dimension	Ψ_6	Ψ_4	*g(r)* at the first peak
10 mM	5.5	1.808	0.045	0.039	3.6
10 mM	10	1.846	0.117	0.039	3.8

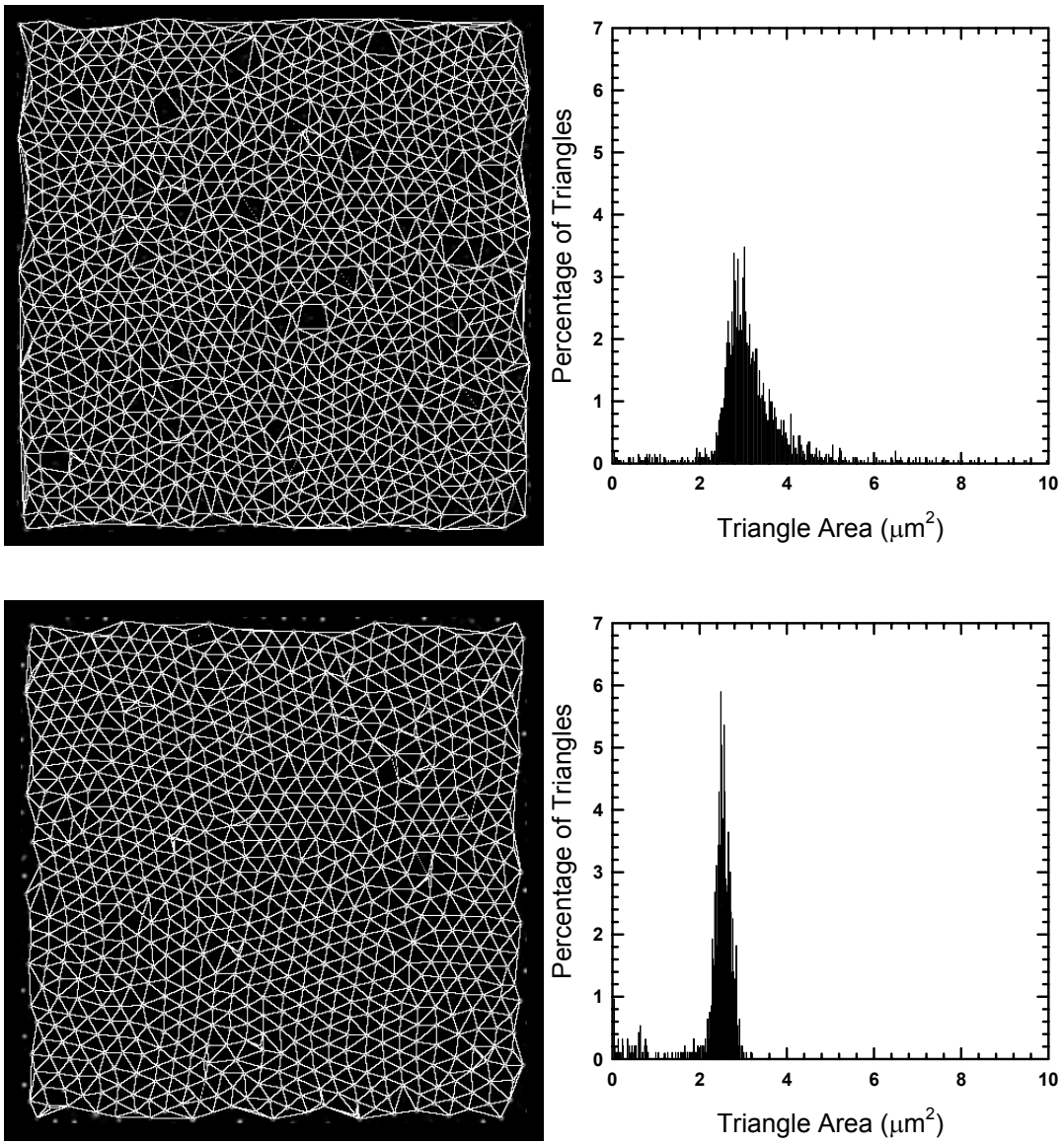

Figure 5.3. Triangulation histograms for pH =5.5 (Top) and pH = 10 (Bottom) clearly show a sharpening of the peak. The triangulated images also clearly indicate an increase in the order in the surface layers as the pH is increased.

Both CLSM experiments performed were in the reaction-limited regime. The difference is the higher repulsive barrier at pH 10 than at pH 5.5. A direct consequence of this is that particles have a longer surface diffusion time t_{diff} at a pH of 10 than at pH of 5.5. The TIRM experiments confirm that $t_{diff\ (10)} > t_{diff\ (5.5)}$. The natural consequence

of these increased diffusion times is the higher order in surface layers of deposited colloidal silica at pH 10 as compared to pH 5.5. This is confirmed by the values of fractal dimension and bond-orientational order parameter reported in the previous section. Radial distribution functions as well as triangulation studies reveal the same information. A direct result of these studies is the understanding that while reaction limited regime deposition gives structures with higher order, careful variation of repulsive energy barrier within this regime can yield structures with even higher order.

5.3.2 Measurement of pH dependent deposition and structure on silica substrates (TIRM studies)

The purpose of the TIRM study was to get a complete understanding of the interaction-surface structure relationship. By knowing exactly what repulsive barrier height leads to higher surface structure, reproducible results are made more likely. TIRM analyses were performed for both the 5.5 as well as the 10 pH case (both at 10mM) in an attempt to understand the kind of interactions in the reaction limited regime and the dependence of these interactions on solvent conditions.

The interaction profile is easily determined for the pH 10 case. The interaction potential at pH 10 is recorded and reported in this research section. This directly gives the interactions in colloidal systems in the reaction-limited regime (Figure 5.4). The interaction potential reported is in terms of relative separation. The part of the curve after about 50nm represents the gravitational interaction while the part after 0nm represents the electrostatic repulsion. It is important to emphasize that we accurately know these values and this makes further analyses much more elegant and easy.

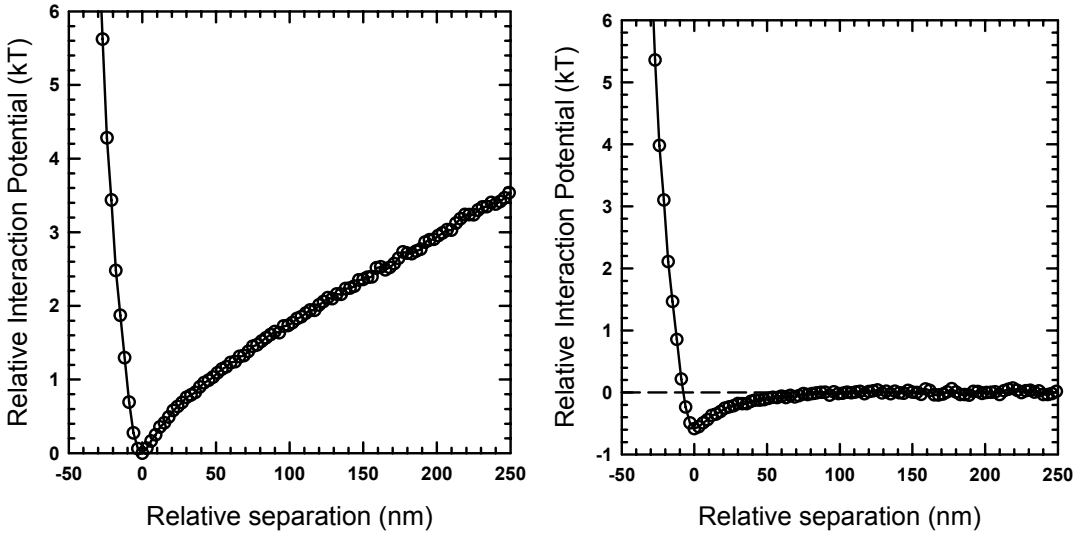

Figure 5.4. The interaction potential between a 2.34 μm silica particle and a glass substrate at 10mM NaCl and pH 10 in terms of relative separation (nm) with (L) and without gravity (R).

The TRIM analysis of the system at 10mM salt and pH 10 directly gives the actual particle wall interaction potential in the reaction-limited regime. The only problem is that the initial results are reported in terms of relative separation. An accurate representation of this interaction potential as a function of absolute separation would be most useful. For this purpose it is very important to find the absolute separation at minimum potential energy. A MathCAD document written in the research group was used for this purpose. The absolute separation curve is shown in Figure 5.5.

The curve in Figure 5.5 and the gray curve in Figure 5.1 have the same nature. The reason the entire barrier and the deep primary minimum are not seen in Figure 5.5 is that the particle does not sample those positions when it is levitated. Those positions are sampled when it is in the process of overcoming the potential energy barrier.

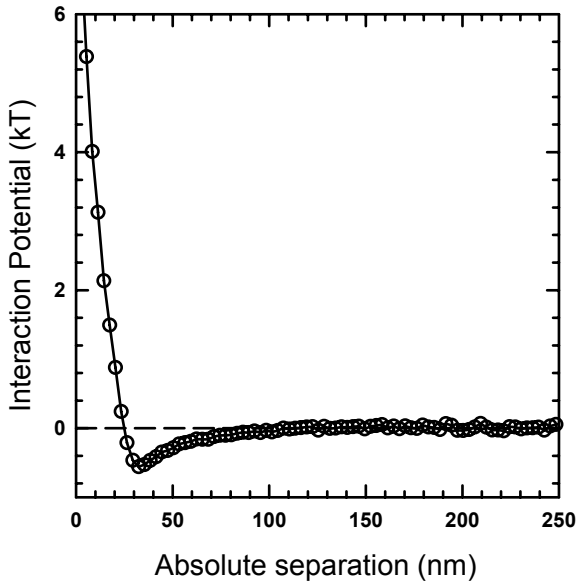

Figure 5.5. The interaction potential between a 2.34 μm silica particle and a glass substrate at 10mM NaCl and pH 10 in terms of absolute separation (nm).

5.4 Conclusions

This research section revealed two important pieces of information. Reaction limited deposition results in the formation of higher ordered structures as compared to the diffusion limited deposition case (Figure 5.6). The second important piece of information is that if the repulsive barrier height is increased such that the new barrier height is still surmountable then the system forms structures with even greater order while still remaining in the reaction limited regime. Another important observation is that all structures formed in this section are irreversible.

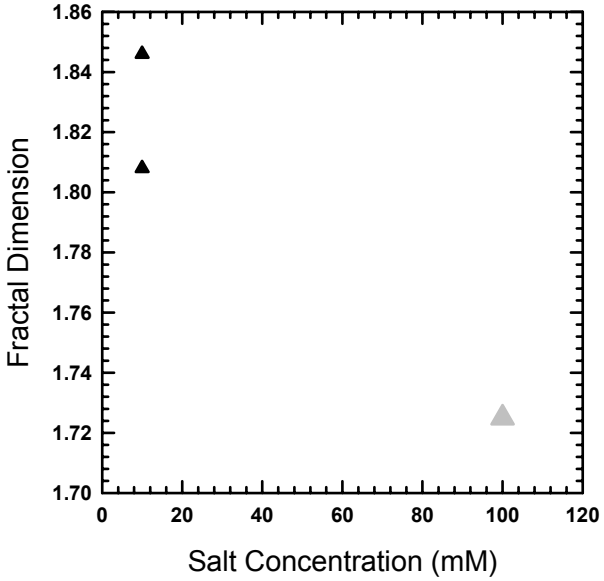

Figure 5.6. Reaction limited deposition structures (black triangles) show higher values of fractal dimensions than structures formed by diffusion-limited deposition (gray triangle).

6. LEVITATION & DEPOSITION WITH POLYMERIC FORCES

6.1 Introduction

In this part of the study we show how TRIM can be used to obtain a fundamental understanding of polymeric stabilization. Adsorbed polymer layers generate repulsion analogous to a hard wall. Under certain solvent conditions, the adsorbed polymer layers are thick enough to generate repulsion of sufficient range and magnitude to dominate van der Waals attraction.[7] The thickness of these adsorbed polymer layers depends on the solvent conditions and the properties of the underlying substrate. The changes in polymer layer thickness brought about by variation in solvent conditions are reversible.

In this research section the influence of hydrophobicity/hydrophilicity of substrates on the interaction potential is studied (depth of the attractive well and position of potential energy minima). This is a direct result of the thickness of the F108 Pluronic layers being dependent on how hydrophobic/hydrophilic the underlying substrates are. F108 is a triblock copolymer of the B/A/B type where the anchor block (A) is strongly attracted to the surface while the buoy blocks (B) are not.[46,47] The B blocks are hydrophilic and as a result, they stretch out further into the solvent as the substrate becomes more and more hydrophobic. The influence of substrate chemistry on adsorbed polymer layer thickness is studied using both TIRM and CLSM techniques.

TIRM experiments for various surface chemistries namely polystyrene (PS) and octadecyltricholorosilane (OTS) are conducted. Since OTS is more hydrophobic than PS, the adsorbed polymer layers must be thicker on OTS than on PS. The results obtained in this section verify the theory. The other experiments in this section involve the use of specific ions to control the polymer layer thickness and achieve bulk phase aggregation and deposition. CLSM analyses are conducted to find out the packing order in diffusion limited deposition regime.

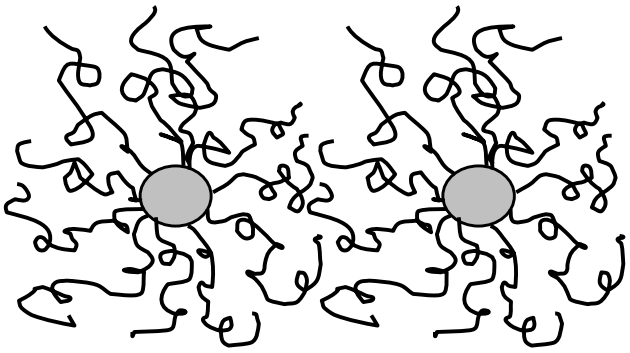

Figure 6.1. Polymeric stabilization. The polymer layers generate a hard wall repulsion of sufficient range to dominate core particle van der Waals attraction under good solvent conditions.

6.2 Theory

6.2.1 Polymeric stabilization

Figure 6.1 schematically depicts the physical arrangement involved in polymeric stabilization of colloidal particles. Under good solvent conditions, the polymer layers are highly solvated and therefore have dielectric properties that are similar to the medium and contribute a minimal amount to the van der Waals force. The adsorbed polymer layers generate repulsion analogous to a hard wall. To stabilize particles, adsorbed polymer layers must be thick enough to generate repulsion of sufficient range and magnitude to dominate van der Waals attraction. [7]

In the event that a polymerically stabilized dispersion experiences a change from good solvent conditions for the adsorbed layer, a dimensional collapse and densification of the adsorbed polymer layers increase the polymeric van der Waals contribution. This dimensional collapse can result is aggregation of the colloids in the event that the range of the van der Waals interaction exceeds the composite particle collision radius. It has been shown that a change back to good solvent conditions results in re-dispersion of the colloids.[30] The objective is to evaluate surface structure at conditions corresponding to complete layer collapse. Another goal is to use a combination of bulk phase aggregation

results, past group research work and fundamentals learnt from the previous chapters to isolates various deposition regimes in these systems.

6.2.2 Silica surface modification using silane chemistry

The space between homogeneous phases is sometimes called the interphase. In this region there is a steep gradient in local properties of the system. By treating a substrate with silanes, the interphase can acquire specific surface energy, partition characteristics, mechanical and chemical properties. Alkyl- and aryl-silanes are non-functional materials that have profound effects of the interphase. They are used to alter surface energy or wetting characteristics of the substrate. For example, glassware can be dipped into a 5% to 10% solution of dimethyldiethoxysilane and heated for ten minutes at 120^{o}C to render the surface hydrophobic.

Silanes can alter the critical surface tension of a substrate in a well-defined manner. Critical surface tensions are associated with the wettability or release qualities of a substrate. Liquids with a surface tension below the critical surface tension (γ_c) of a substrate will wet the surface, i.e., show a contact angle of 0 ($\cos\theta_c = 1$). The critical surface tension is unique for any solid, and is determined by plotting the cosine of the contact angles of liquids of different surface tensions and extrapolating to 1. The contact angle is given by Young's equation:

$$\gamma_{sv} - \gamma_{sl} = \cos\theta_e \qquad (6.1)$$

where γ_{sl} = interfacial surface tension, γ_{lv} = surface tension of liquid, and $\gamma_{sv} = \gamma_l$ when $\gamma_{sl} = 0$ and $\cos\theta_e = 1$. OTS will be used in this research section to make glass surfaces hydrophobic.[48]

6.2.3 Specific ion effect

Exquisite control of the interparticle potential can be obtained by reversible and continuous control of the balance of attractive dispersion forces and molecular interactions between polymer-coated colloids using specific ion effects. The classic study by Napper on the effects of different electrolytes on the fractal aggregation of

polystyrene latexes coated by polymers is the basis for this study. The study states that poly (*N*-isopropylacrylamide)(PNIPAM) is soluble in water at low temperatures, but on addition of electrolyte, it adopts a globular conformation and becomes hydrophobic. The effect is also dependent on the type of salt used.[5,49,50]

6.3 Experimental

6.3.1 Materials

Nominally sized 4.9μm polystyrene colloids purchased from Interfacial Dynamics Corporation were used in these experiments. Sodium chloride (NaCl), used to control the ionic strength in these experiments was purchased from Aldrich and used without purification. F108 Prill Pluronic was purchased from BASF for use in the experiments. The OTS used for chemical surface modification was purchased from Avocado Research Chemicals Ltd. The Toluene (Histological Grade),used as a solvent for the OTS was purchased from Fisher Scientific and used without purification. 20mm x 20mm zinc titania glass cover slips (SiO_2 64%, B_2O_3 9%, ZnO 7%, K_2O 7%, Na_2O 7%, TiO_2 3%, Al_2O_3 3%)(Corning) were used as substrates in the deposition experiments.

6.3.2 Cell preparation

The colloidal deposition was carried out in sedimentation cells. The cells used for the deposition experiments involving the polymer coated particles were constructed by attaching 1mm x 10mm (*h x id*) O-rings to 20mm x 20mm cover slips (Corning) using polydimethyl siloxane (PDMS, Sylgard 184, Dow Corning). The sedimentation cells were always covered with another 20mm x 20mm cover slip to avoid evaporation. Vacuum grease was used to seal the top cover slip onto the O-ring or pipe piece. The cover slips were cleaned by immersing them in Nochormix overnight and then washing them repeatedly in de-ionized water. The cover slips were dried in a stream of nitrogen gas.

The PS particles were levitated above the flat PS surface by adsorbing layers of Pluronic onto both surfaces. Pluronic was adsorbed onto the particles by shaking them in a 1000ppm polymer solution for 16 h. The bulk concentration of 1000ppm is at least three times the concentration necessary to saturate the PS surfaces. The particles were then diluted such that they finally were part of a 0.5M NaCl solution that was polymerically stabilized.

6.3.3 Surface modification with PS

Glass slides that had been cleaned as described earlier were spun at 1000rpm for 60 s with a 10 wt % solution of PS in toluene. The spin coated surface was then annealed in an oven at 120^{o}C for 16h before being brought to room temperature. The O-rings were then stuck on these PS surfaces as described earlier. Polymer was adsorbed on these surfaces by placing a 85μL of the 1000ppm polymer solution on them for about 16 h. Before the start of the experiments the drop was sucked off the surface.[29,30]

6.3.4 Surface modification with OTS

Microcontact printed OTS solution films were obtained by spin-casting a 10mM solution of OTS in toluene onto a polydimethylesiloxane(PDMS) stamp using a conventional photo resist spinner at 3000 rpm for 30s. A spinner was used to apply the solution uniformly without the risk of contaminating the surface with particles. The wetted PDMS stamp was then dried in a steam of nitrogen gas for 30s, after which it was brought in contact with the substrate for 30s.[24] The PDMS stamps used for the planar microcontact printing were fabricated according to a previously reported procedure. The O-rings were then stuck on these OTS surfaces as described earlier.[51] Polymer was adsorbed on these surfaces by placing a 85μL of the 1000ppm polymer solution on them for about 16 h. Before the start of the experiments the drop was sucked off the surface.[29,30]

6.3.5 TIRM studies

A Hamamatsu *ORCA-ER* C.C.D. camera was used to capture images of the sample over the surface. The particle scatters an evanescent wave produced by total internal

refection of a 543 nm He-Ne laser. The solutions of 0.5M concentrations were prepared by diluting the original polymers coated solution of PS spheres with a 1M NaCl solution.

6.3.6 Confocal imaging

A Ziess confocal scanning laser microscope was used to image the first layer of all the deposited structures. The microscope was operated in reflection mode using a 633 nm He-Ne laser. The pinhole was always kept at 1 airy unit. Images were taken at various zoom values. Images were taken at various zoom values. Images are taken at zoom values of 0.7 (pixel/μm = 0.4), 1(pixel/μm = 0.29), 1.7(pixel/μm = 0.17) and 2.7(pixel/μm = 0.11).

6.3.7 Procedure

The TRIM experiment involved varying the nature of the underlying homogenous substrate and recoding the interaction potential and polymer layers thickness. The analyses were performed for two different systems. The first was for PS spheres with adsorbed polymer interacting with a PS surface with adsorbed polymer at 0.5M NaCl. The second experiment was for PS spheres with adsorbed polymer interacting with an OTS surface with adsorbed polymer at 0.5M NaCl.

The second set of experiments in this section involved studies on bulk stability of these systems. CLSM analysis of surface layer at 0.5M magnesium sulfate was performed. Using past group data and knowledge form earlier sections in this research, isolation of diffusion limited and a reaction-limited regime is possible.

6.4 Results and discussion

6.4.1 Effect of substrate properties on polymeric stabilization. (TRIM studies)

TRIM experiments were performed for PS colloids interacting with two kinds of substrates: PS and OTS. The particle wall interaction potential is determined for both cases as is the polymer layer thickness. It is clearly seen that the well depth for the PS-PS system is greater than for the PS-OTS system. Table 6.1 and Figure 6.2 serve to illustrate the point made.

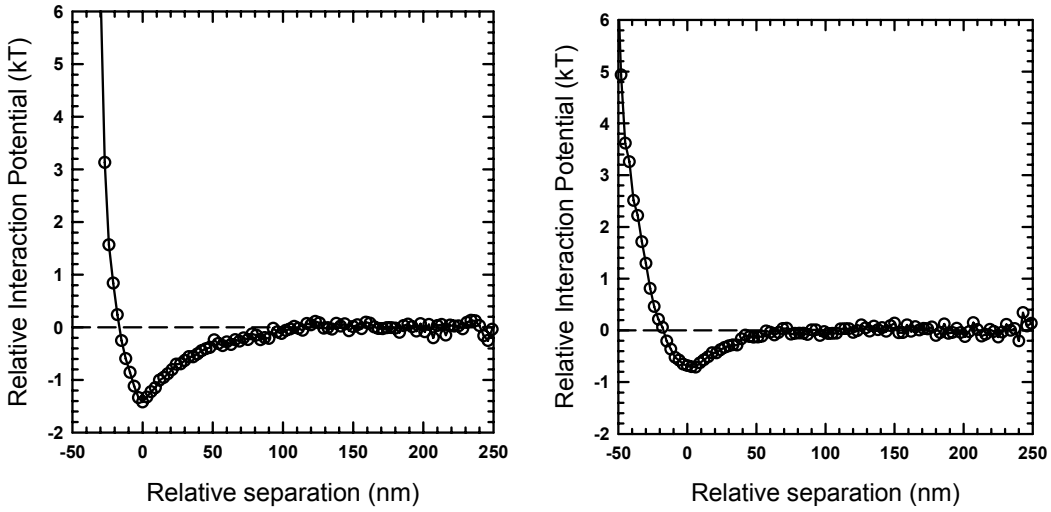

Figure 6.2. (L-R) Interaction potentials for PS-PS and PS-OTS cases clearly show a decrease in the attractive well depth. This is attributed to OTS surface being more hydrophobic than PS (resulting is thicker polymer layers).

Table 6.1 Influence of underlying substrate chemistry on the attractive well depth in polymerically stabilized systems

Type of system	Attractive well depth (kT)
PS-PS	-1.6 kT
PS-OTS	-0.8 kT

The other important piece of information that was backed out from the TRIM data was the polymer layer thickness on the underlying substrate. The high salt concentrations used ensured that the electrostatics were absent in these systems. The only interactions in this system were the van der Waals attraction and the polymeric hard wall repulsion. It is assumed that the minimum potential energy position lies at the point of contact of the adsorbed polymer layers. At separations closer than this the hard wall repulsion generated by the polymer layers pushes the particles apart. A simple MathCAD Document is written to determine the absolute separation and minimum potential energy separation.

The curve fitting for the raw data for both PS-PS as well as PS-OTS is shown in Figure 6.3. The theoretical curves are of the form:

$$f(x, hm) = (ae^{-bx}) + (y + cx) + d(x + hm)^e \qquad (6.2)$$

where ae^{-bx} is the fitting done to the repulsive part of the profile, and $y + cx$ is the fitting to the gravitational part of the profile. d and e are the coefficients obtained from the power law fit to the van der Waals data given by Eq.(2.4). x represents the relative separation is nm and hm is the value of absolute minimum potential separation, which has to be found out.

There are some differences in the coefficients in these equations. The linear parts of the curve (gravity) have different intercepts and slopes. The difference in slopes is due to particle polydispersity. The difference in the intercepts is due to a variety of reasons. Gravitational interaction is relative to zero separation and since the raw data is obtained as a function of relative separation, an intercept is obtained. The other important cause is that the minimum separation sampled in the two cases is different. This is attributed to the difference in polymer layer thickness, which will be explained later.

The values of hm for which the fits are obtained, represent the minimum separation sampled by particles in those systems. As stated earlier, the thickness of the adsorbed polymer layers is determined from this analysis. Figure 6.4 shows the relevant separations defined in the TRIM experiments with polymeric stabilization. On contact $h = hm = 2\delta$ and $x = 0$. It is assumed that the particle and the substrate are the same material. This applies directly to the PS-PS case. The value of hm here is 45nm, which results in the polymer layer thickness on the substrate being 22.5nm. Pluronic adsorbed on PS surfaces therefore forms layers of thickness 22.5nm at a pH of 5.5, ionic strength of 0.5M and temperature of 25^{o}C. The value of hm for the OTS-PS case is 52nm. Since the polymer layer thickness on PS is already known, the OTS polymer layer thickness is 29.5nm.

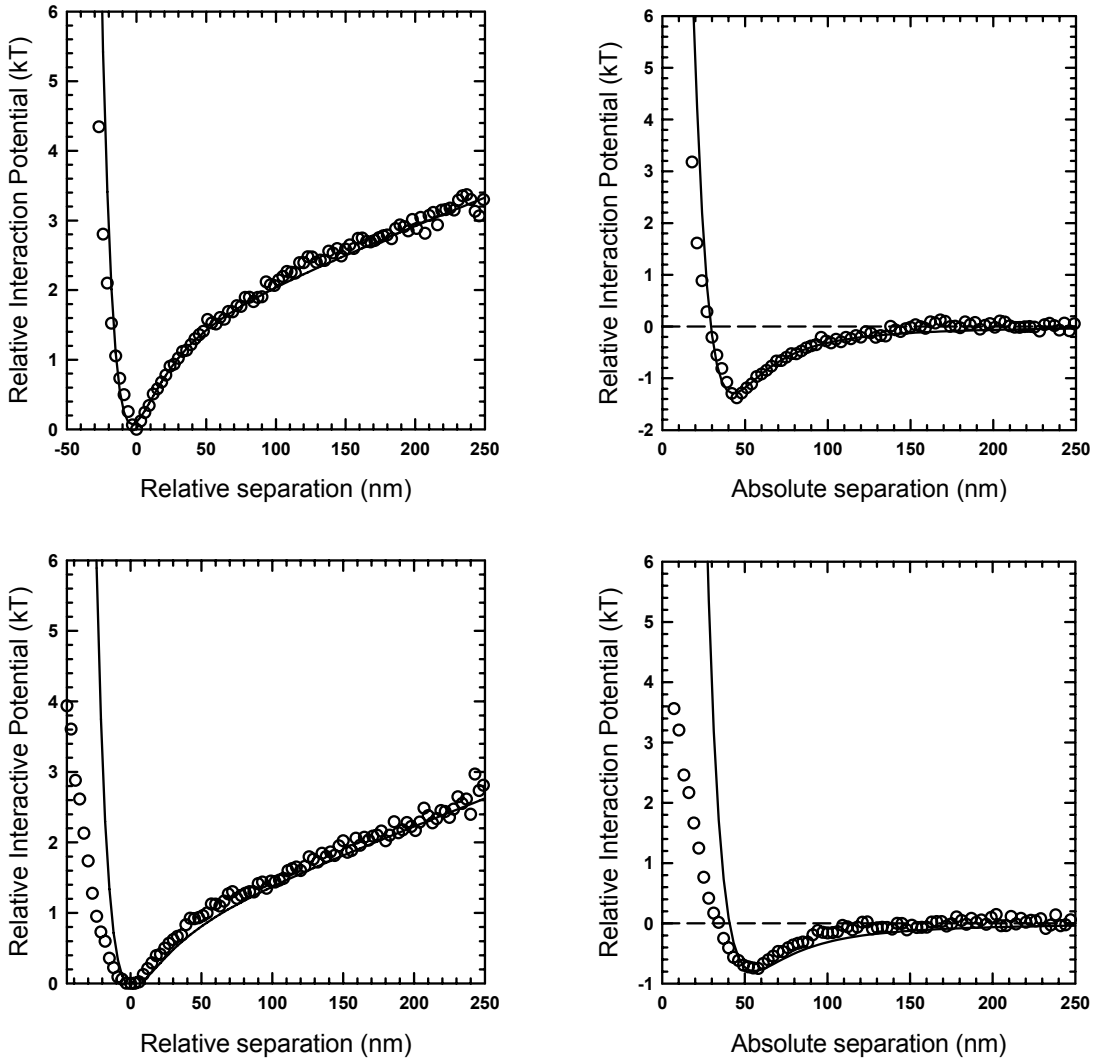

Figure 6.3. (Top) Fitting for the PS-PS interaction data with gravity (L) and without (R). The value of hm for the fit shown is 45nm. (Bottom) Fitting for the PS-OTS interaction data with gravity (L) and without (R). The value of hm for the fit shown is 52nm.

The explanation for the change in adsorbed polymer layer thickness and the depth of the attractive well lies in the properties of the adsorbed polymer and those of the underlying substrates. F108 is a triblock copolymer of the B/A/B type where the A block is strongly attracted to the surface while the B blocks are not.[46] The B blocks are hydrophilic and as a result, they stretch out further into the solvent as the substrate

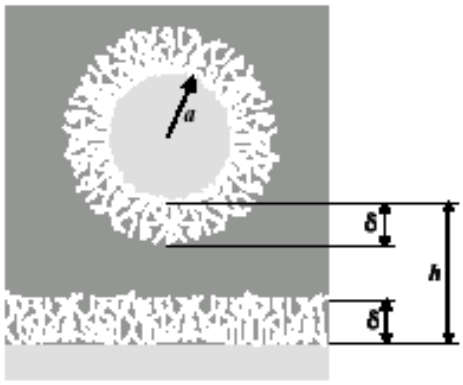

Figure 6.4. The relevant separations in polymeric stabilization showing layer thickness and bare surface separation.

becomes more and more hydrophobic. PS surfaces are hydrophobic and as a result the hydrophobic PPO block lies flat on the surface whereas the hydrophilic PEO tails stretch out into the solvent. OTS surfaces are even more hydrophobic than PS. This is clearly evident form the critical surface tension values for both surfaces (PS: 33-43 dyne/cm & OTS: 25.9-27 dyne/cm). The result states that at fixed solvent conditions, variations of substrate chemistry, change interactions in polymerically stabilized systems. Tables 6.2. & 6.3. summarize all the results. Changing the polymer layer thickness shifts the hard wall repulsion. This is easily seen in Figure 6.5.

Table 6.2 Influence of substrate chemistry

Type of substrate	Critical surface tension (dyne/cm)	Thickness of adsorbed polymer on substrate	Attractive well depth (kT)
Polystyrene	33-43 dyne/cm	22.5 nm	-1.6 kT
OTS	25.9-27 dyne/cm	29.5 nm	-0.8 kT

Table 6.3 Influence of substrate properties

Type of substrate	a	b	y	c	d	e
PS	0.68	0.13	1.38	0.0079	-11802.81	-2.287
OTS	0.62	0.12	0.7223	0.0077	-11802.81	-2.287

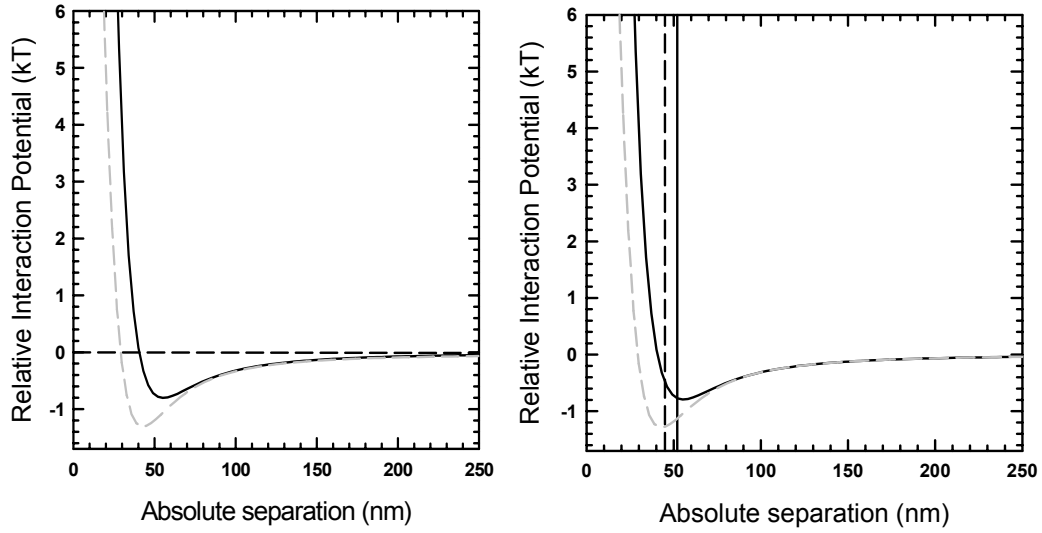

Figure 6.5. Interaction potentials for PS-PS (gray dash) and PS-OTS (black) showing the shifting of hard wall repulsion.

6.4.2 Predicting diffusion limited deposition and aggregation

Aggregation is caused by attractive wells of 5-10kT.[8] From previous group research, the polymer layer thickness at 0.5M $MgSO_4$ is found to be 5nm(on both PS or OTS). The hard wall position in terms of interparticle separation is therefore 10nm. On Figure 6.6, this defines a well depth of about 24kT (black dashed line). The van der Waals curve in Figure 6.6 is generated from Eq.(2.3) with the necessary adjustments for particle size. We can therefore predict that at 0.5M $MgSO_4$, a bulk suspension of polymer coated PS particles will undergo aggregation. A system of polymer coated PS spheres interacting with a polymer coated PS surface is expected to undergo rapid deposition. The predictions are supported by both the bulk aggregation observations and the deposition results.

Preliminary experiments were conducted to test the stability of polymerically stabilized PS particles with increasing amounts of $MgSO_4$. The results show that while the system is stable at 0M and 0.25M MgSO4 (and total salt concentration of 0.5M), aggregates form at 0.5M $MgSO_4$ concentrations (Figure 6.7). The purpose of this study

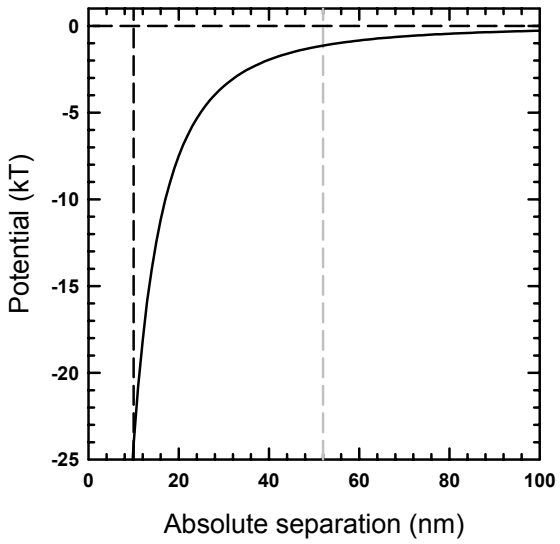

Figure 6.6. Predicting rapid-deposition from particle-wall interaction potential. The red line represents position of hard wall at 0.5M $MgSO_4$ (showing a deep attractive well of 24kT) and the blue line represents the position of the hard wall at 0.5M NaCl.

is to isolate diffusion limited kinetics regime in these systems from a fundamental understanding of the interactions involved. Group data on specific ion effects shows that at 0.5M $MgSO_4$, the polymer layers collapse totally, resulting in a system with only van der Waals attraction.

Experiments with polymer coated PS particles and a polymer coated PS slide at 0.5M $MgSO_4$, reveal the deposition process to be diffusion limited. The resulting structures, when analyzed with CLSM (light gray triangles in Figure 6.8), show the same characteristics (*g(r)* profile and fractal dimension) of previous diffusion-limited deposition structures. The dashed gray line on Figure 6.6 represents the hard wall at 46 nm that corresponds to the PS-OTS system at 0.5M NaCl.

Figure 6.7. Bulk aggregation experiments performed at (L-R) 0.5M NaCl, 0.25M NaCl+0.25M $MgSO_4$ and, 0.5M $MgSO_4$ clearly showing aggregation at 0.5M $MgSO_4$ as predicted.

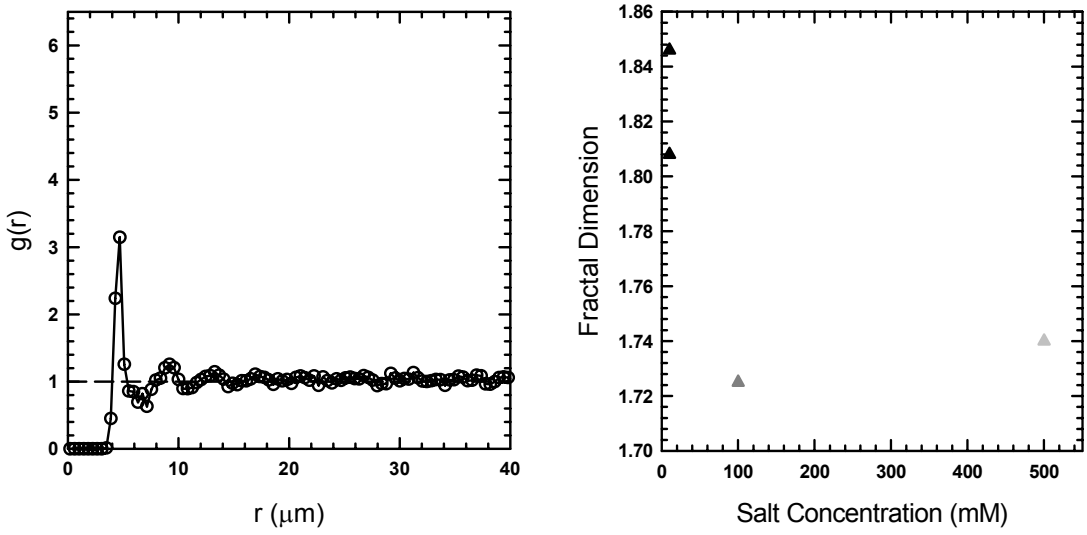

Figure 6.8. (L) Surface structure (represented by g(r)) for a PS particle on OTS diffusion limited deposition structure showing the typical random nature of such structures. (R) The fractal dimension of surface structures formed by rapid deposition kinetics is independent of the chemical nature of the system. The light gray triangles are results for rapid deposition of polymer coated PS particles on polymer coated substrates and the dark gray triangles are results for rapid deposition of silica particles on silica substrate.

6.5 Conclusion

In this final research section, we have successfully shown that, detailed knowledge of interaction potential between particles (aggregation) or between particle and wall (deposition) is enough to predict the advent of diffusion-limited kinetics. This section has also analyzed the effect of substrate chemistry on interactions in polymeric systems. The result of change in substrate chemistry is a shift in the position of hard wall repulsion.

7. CONCLUSIONS

7.1 Summary

In the course of this research work, we have shown that large amounts of attraction lead to the formation of disordered states irrespective of the nature of the interaction. We have also demonstrated the importance of repulsive barrier height in the assembly of two-dimensional structures with higher amounts of order. We have successfully predicted solvent conditions that result in diffusion limited deposition from the fundamental interaction potential for polymeric systems. TIRM measurements of interactions in such polymerically stabilized systems have been conducted and the influence of surface chemistry on the interactions has been studied.

Using various analysis techniques including fractal dimension, bond-orientation order, radial distribution function and triangulation, it has been demonstrated that large attractive particle-particle and particle-wall interactions yield disordered structures. This was found to be true for any kind of attractive interaction. The conditions resulting from such high amounts of attraction were not at all conducive to building structures with long-range order. Experiments were therefore conducted in the "reaction-limited" regime, which requires that a substantial but surmountable repulsive barrier be present to allow particles the necessary time to form ordered structures. The surface diffusion time allowed was controlled by modification of the surface charge on the particles. It was found that an increase in the surface charge/repulsive barrier height led to much longer surface sampling times which in turn led to the formation of structures with slight improvements in order.

The switch to polymerically stabilized systems was made keeping in mind the irreversible nature of the deposition process in charge-stabilized systems. Past studies have demonstrated the reversible nature of aggregation in polymerically stabilized systems.[6] A brief study on the effect of substrate hydrophobicity on adsorbed polymer layer thickness/depth of attractive well was conducted. It was observed that increasing the hydrophobic nature of the substrate made the polymer brush thicker and the well

shallower. The final studies conducted involved the effect of specific ions on the interactions in these systems.

The effect of increasing specific ion concentrations on the two dimensional order of colloidal structures was conducted. The universality that exists in colloidal aggregates does exist is deposited structures as well. The similar structural characteristics shown by three chemically different systems, all under diffusion limited deposition kinetics, justifies this claim.

8. FUTURE RESEARCH

8.1 Diffusing colloidal probe microscopy (DCPM)

DCPM is a novel method of imaging surfaces. Past studies have used scanning force microscopy (SFM) with chemical specificity to do chemical imaging of surface functional groups.[52] These studies involved chemical modification of the SFM probe with functional groups that provide a specific interaction with the functional groups of interest on the sample surface. Relationships between friction and adhesion forces were used to image up to three different functional groups on the same surface.[52] Other studies have used atomic force microscopes to measure interactions between a sphere glued to its tip and a surface.[53] The drawback of all these methods is the sensitivity. TIRM is many orders of magnitude more sensitive than the previously used methods.[34]

As shown in this research, TIRM can be used to accurately measure the interaction between a PS colloid and OTS surface, both with adsorbed layers of polymer on their surface. The research also obtained data for the influence of substrate chemistry on adsorbed polymer layers thickness and particle-substrate interactions. It was found that on increasing the hydrophobicity of the substrate, the thickness of the adsorbed polymer layer increased and the interaction profile changed. In this research we only looked into homogeneous surfaces. If experiments were performed on heterogeneous surfaces, we would expect to see some particles having different interactions than others depending on their surface positions. The difference in interaction potentials can be used to image the surface.

Some initial experiments have been attempted in this direction. This experimental work is being done in collaboration with Hung Jen Wu. We tried to see if this technique could be applied to the simplest of heterogeneous surfaces. By microcontact printing OTS onto one half of the cover slip we made a surface that was heterogeneous but yet simple as shown in Figure 8.1. The part with the OTS monolayer on it was hydrophobic whereas the part with bare silica was hydrophilic. It is easy to imagine that when polymer is adsorbed to this surface, there will be a noticeable

difference in the layer architecture depending on where the layers attach. The polymer will lie flat on the silica part but will extend out into the liquid on the OTS region. Thus, depending on their position, particles will experience different interactions with the surface. By knowing the position specific interactions, we can easily obtain a potential energy profile of the surface.

8.2 Specific ion effects on polymer mediated interfacial structures

In this research a few results for interaction potentials of polymer-coated colloids with polymer-coated OTS surfaces have been reported. Initial studies into the structural effects of addition of specific ions have been conducted. A detailed measurement of the interaction potentials at a number of specific ion concentrations needs to be done. This will help to better understand the nature of the structures being formed by deposition. The objective here is to identify conditions producing an attractive minimum just sufficient to cause phase separation and avoid flocculation. It is known that flocculation occurs when the interparticle potential changes from purely repulsive to strongly attractive with a minimum deeper than –5kT to –10kT. Phase separation on the other hand requires a well attraction of –1kT to –5kT.[8] The measurements conducted in this research show that at 0.5M NaCl, the particle-particle wells are about -0.7kT. The particle-OTS interaction is –0.8kT. A subtle change in the potential is all that is required to induce phase separation. This will therefore be a very exciting research avenue for the future.

To further motivate this research, initial work has already been done on these systems.[7] Figure 8.2. is a summary of past work done by Dr.M.A.Bevan. He has rheologically determined the fluid-gel transition for a fixed polymer layer thickness and core radius but with varying particle volume fraction. The solid lines in the figures were constructed adhesive sphere potentials. By TIRM we can directly measure the interaction potential. At 25^{o}C and a fixed volume fraction on the phase diagram, we can manipulate the attraction by use of specific ions to obtain phase transition.

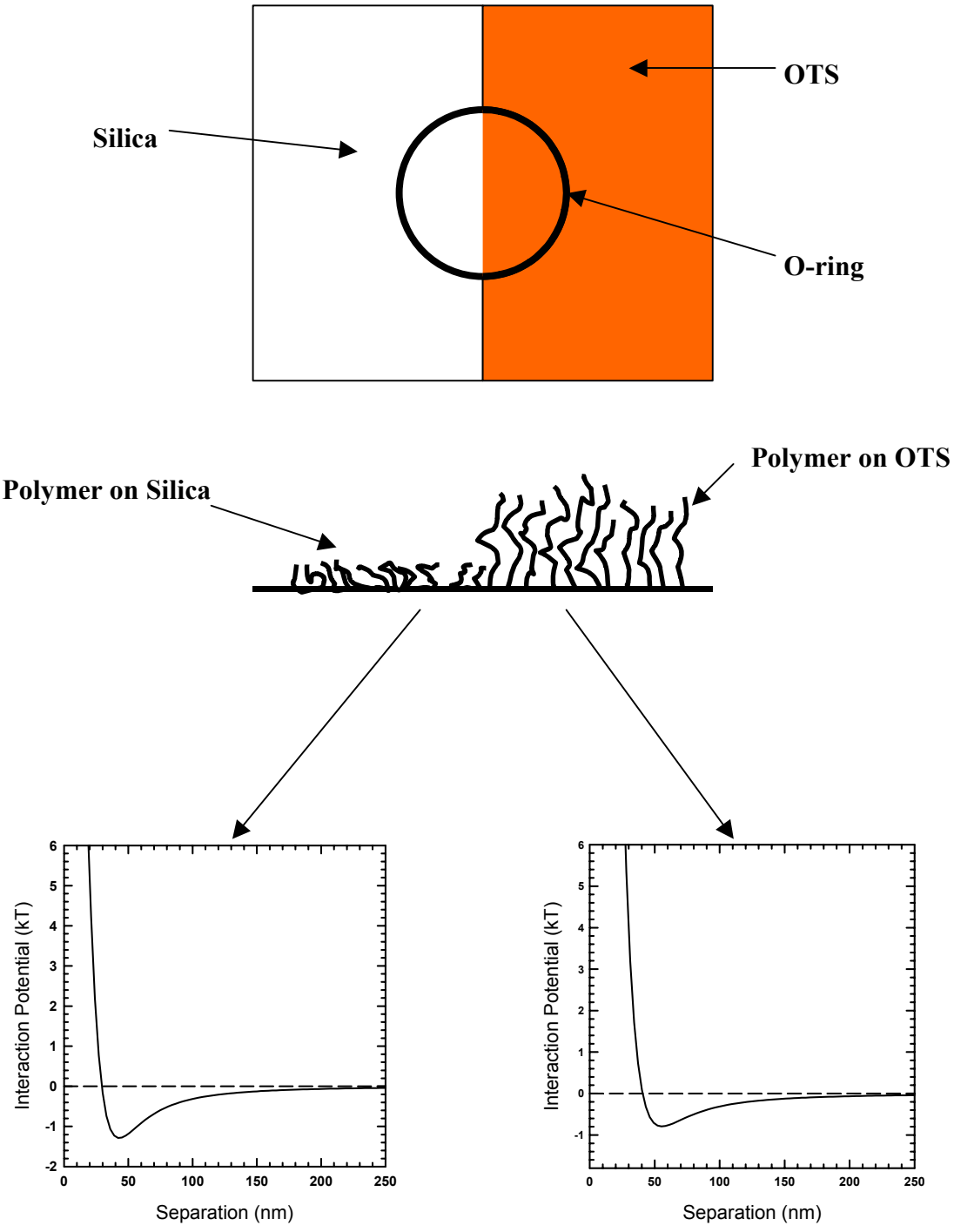

Figure 8.1. Diffusing Colloidal Probe Microscopy (DCPM) on a simple heterogeneous surface.

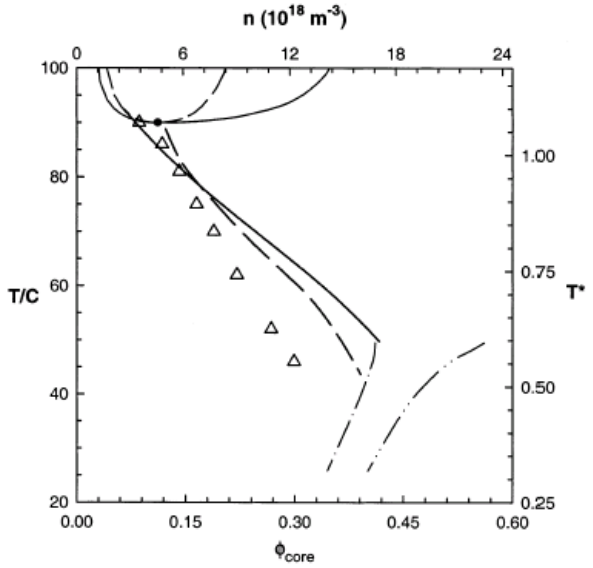

Figure 8.2. Previous work on phase transition in polymerically stabilized systems.[7]

8.3 Manipulation of self-assembly on chemical templates

In order to control the orientation of adhesive colloidal crystals we plan to tune interactions between colloids and chemical templates. The basic data form measurements carried out on homogeneous surfaces will be useful here. This research work has already use microcontact printing for modifying glass surfaces. The only difference will be the switch from the planar stamps used in this research to stamps with intricate patterns.

Combinations of charged and neutral silanes can be used to generate electrostatic potential energy templates.[26] Adsorbing pluronics on silane patterns of varying degrees of hydrophobicity will be used to create laterally varying layers with thick brush and thin brush for deposition of polymer coated particles.[54] The colloid-template interaction can then be tuned sensitively and reversibly by using a combination of temperature and specific ion effects. Problems with visualization of the silanes can be countered by the

use of fluorescent dyes. These can be adsorbed to the silanes before microcontact printing is done.

8.4 Protein interaction measurements

The Tar Chemoreceptor of the *E.Coli* is one of the most thoroughly studied membrane proteins. Interaction of ligand bound MBP with Tar enhances counterclockwise flagella rotation to favor smooth swimming and migration of cells towards higher maltose concentrations. Because the MBP-Tar interactions is an example of a specific biomolecular interaction that cannot be observed or quantified with existing technologies, a DCPM method will be ideal for directly probing specific biomolecular interactions on the order of kT. The experiment will be involve covalently attaching the MBP molecule to 5-10 nm gold nanoparticle surfaces and watching its interactions with a flat supported lipid bilayer.

8.5 Combinatorial microarray experiments

Microarray techniques allow simultaneous detection of the presence or absence of many combinations of biomolecules in a single experiment. The current techniques for probing "microarrays" require large sample amounts and large feature sizes, which waste precious sample. Ensembles of levitated colloidal probes will dramatically improve the sensitivity and rate at which specific biomolecules are detected on high information density nanoarrays. The success of this research depends on the success of the DCPM techniques on simple synthetic polymer heterogeneous surfaces mentioned in the earlier paragraphs.

REFERENCES

(1) Lin, M. Y.; Lindsay, H. M.; Weitz, D. A.; Ball, R. C.; Klein, R.; Meikin, P. *Nature* **1989**, *339*, 360.

(2) Robinson, D. J.; Earnshaw, J. C. *Physical Review A* **1992**, *46*, 2045.

(3) Robinson, D. J.; Earnshaw, J. C. *Physical Review A* **1992**, *46*, 2055.

(4) Robinson, D. J.; Earnshaw, J. C. *Physical Review A* **1992**, *46*, 2065.

(5) Napper, D. H. *Polymeric Stabilization of Colloidal Dispersions*; Academic Press: New York, 1983.

(6) Bevan, M. A.; Prieve, D. C. In *Polymers in Particulate Systems: Properties and Applications*; Hackley, V. A., Somasundran, P., Lewis, J. A., Eds.; Marcel Dekker: New York, 2001; Vol. 104.

(7) Bevan, M. A.; Petris, S. N.; Chan, D. Y. C. *Langmuir* **2002**, *18*, 7845.

(8) Russel, W. B.; Saville, D. A.; Schowalter, W. R. *Colloidal Dispersions*; Cambridge University Press: New York, 1989.

(9) Evans, D. F.; Wennerstrom, H. *The Colloidal Domain*; 2nd ed.; Wiley-VCH: New York, 1999.

(10) Russel, W. B.; Chaikin, P. M. *Nature* **1997**, *387*, 883.

(11) Gast, A. P.; Russel, W. B. *Physics Today* **1998**, *51*, 24.

(12) Pusey, P. N.; Megen, W. v. *Phys. Rev. Lett.* **1987**, *59*, 2083.

(13) Dawson, K. A. *Curr. Op. in Colloid and Interface Sci.* **2002**, *7*, 218.

(14) Witten, T. A.; Sander, L. M. *Physical Review B* **1983**, *27*, 5686.

(15) Forrest, S. R.; Witten, T. A. *J.Phys.A:Math.Gen.* **1979**, *12*, L109.

(16) Meakin, P. *Phys. Rev. Lett.* **1983**, *51*, 1119.

(17) Witten, T. A.; Sander, L. M. *Phys. Rev. Lett.* **1981**, *47*, 1400.

(18) Meakin, P. *Physical Review A* **1983**, *27*, 604.

(19) Kumar, A.; Whitesides, G. M. *Appl. Phys. Lett.* **1993**, *63*, 2002.

(20) Wilbur, J. L.; Kumar, A.; Kim, E.; Whitesides, G. M. *Adv.Mater.* **1994**, *6*, 600.

(21) Xia, Y.; Whitesides, G. M. *Angew. Chem. Int. Ed.* **1998**, *37*, 550.

(22) Younan, X.; Mrksich, M.; Enoch, K.; Whitesides, G. M. *J. Am. Chem. Soc.* **1995**, *117*, 9576.

(23) St. John, P.; Craighead, H. G. *Appl. Phys. Lett.* **1996**, *68*, 1022.

(24) Jeon, N. L.; Finnie, K.; Branshaw, K.; Nuzzo, R. G. *Langmuir* **1997**, *13*, 3382.

(25) Chen, K. M.; Jiang, X.; Kimerling, L. C.; Hammond, P. T. *Langmuir* **2000**, *16*, 7825.

(26) Aizenberg, J.; Braun, P. V.; Wiltzius, P. *Phys. Rev. Lett.* **2000**, *84*, 2997.

(27) Masuda, Y.; Itoh, M.; Yonezawa, T.; Koumoto, K. *Langmuir* **2002**, *18*, 4155.

(28) Bevan, M. PhD Dissertation, Carnegie Mellon University, Pittsburgh, PA, 1999.

(29) Bevan, M. A.; Prieve, D. C. *Langmuir* **1999**, *15*, 7925.

(30) Bevan, M. A.; Prieve, D. C. *Langmuir* **2000**, *16*, 9274.

(31) Bevan, M. A.; Scales, P. J. *Langmuir* **2002**, *18*, 1474.

(32) Prieve, D. C.; Luo, F.; Lanni, F. *Faraday Disc.* **1987**, *83*, 297.

(33) Prieve, D. C.; Frej, N. A. *Langmuir* **1990**, *6*, 396.

(34) Prieve, D. C. *Adv. Colloid Interface Sci.* **1999**, *82*, 93.

(35) Hiemenz, P. C. *Principles of Colloid and Surface Chemistry*; 2nd ed.; Marcel Dekker: New York, 1986.

(36) Israelachvili, J. N. *Intermolecular and Surface Forces*; 2nd ed.; Academic Press: New York, 1992.

(37) Feder, J. *Fractals*; Plenum Press: New York, 1988.

(38) Lattuada, M.; Sandkühler, P.; Wu, H.; Sefcik, J.; Morbidelli, M. *Advances in Colloid and Interface Science* **2003**, *103*, 33.

(39) Hansen, J. P.; McDonald, I. R. *Theory of Simple Liquids*; Academic Press: London, 1986.

(40) Hunter, R. J. *Foundations of Colloid Science*; Oxford Univ. Press: New York, 1987; Vol. 1.

(41) Russel, W. B.; Chaikin, P. M. *Nature* **1997**, *385*, 321.

(42) Forrest, S. R.; Witten, T. A. *J.Phys.A:Math.Gen.* **1979**, *12*, L109.

(43) Skjeltrop, A. T. *Phys. Rev. Lett.* **1987**, *58*, 1444.

(44) Bevan, M. A.; Lewis, J. A.; Braun, P. V.; Wiltzius, P. *Langmuir* **2004**, *submitted*.

(45) Rarity, J. G.; Seabrook, R. N.; Carr, R. J. G. *Proc. R. Soc. Lond. A.* **1989**, *423*, 89.

(46) Li, J.-T.; Caldwell, K. D.; Rapoport, N. *Langmuir* **1994**, *10*, 4475.

(47) Fleer, G. J.; Stuart, M. A. C.; Scheutjens, J. M. H. M.; Cosgrove, T.; Vincent, B. *Polymers at Interfaces*; Chapman & Hall: New York, 1993.

(48) Gelest, I. *Silicon Compounds: Silanes and Silicones*; Gelest, Inc.: Morrisville, PA, 2004.

(49) Napper, D. H. *J. Colloid. Interface Sci.* **1969**, *33*, 384.

(50) Zhu, P. W.; Napper, D. H. *Colloids and Surfaces* **1995**, *98*, 93.

(51) Kumar, A.; Whitesides, G. M. *Appl. Phys. Lett.* **1993**, *63*, 2002.

(52) Vegte, E. W. v. d.; Hadziioannou, G. *Langmuir* **1997**, *13*, 4357.

(53) Kokkoli, E.; Zukoski, C. F. *Langmuir* **2001**, *17*, 369.

(54) Pagac, E. S.; Prieve, D. C.; Solomentsev, Y.; Tilton, R. D. *Langmuir* **1997**, *13*, 2993.

VITA

Gregory Fernandes graduated with a B.E. degree in Chemical Engineering from Mumbai University, India in May 2002. In August 2000, he joined the Department of Chemical Engineering at Texas A&M University as a graduate student.

Gregory Fernandes may be contacted through Dr.Michael Bevan at the Chemical Engineering Department, Texas A&M University, College Station, TX-77843.